EUROPEAN RESPIRATORY *journal*

FLAGSHIP SCIENTIFIC JOURNAL OF ERS

Early View

Original article

TRIM33 prevents pulmonary fibrosis by impairing TGF-β1 signaling

Pierre-Marie Boutanquoi, Olivier Burgy, Guillaume Beltramo, Pierre-Simon Bellaye, Lucile Dondaine, Guillaume Marcion, Lenny Pommerolle, Aurélie Vadel, Maximilien Spanjaard, Oleg Demidov, Arnaud Mailleux, Bruno Crestani, Martin Kolb, Carmen Garrido, Françoise Goirand, Philippe Bonniaud

Please cite this article as: Boutanquoi P-M, Burgy O, Beltramo G, *et al*. TRIM33 prevents pulmonary fibrosis by impairing TGF-β1 signaling. *Eur Respir J* 2020; in press (https://doi.org/10.1183/13993003.01346-2019).

TRIM33 prevents pulmonary fibrosis by impairing TGF-β1 signaling

Pierre-Marie Boutanquoi[1], Olivier Burgy[1,2], Guillaume Beltramo[1,3,4], Pierre-Simon Bellaye[5], Lucile Dondaine[1,4], Guillaume Marcion[1], Lenny Pommerolle[1], Aurélie Vadel[6], Maximilien Spanjaard[1,3], Oleg Demidov[1], Arnaud Mailleux[6], Bruno Crestani[6], Martin Kolb[7], Carmen Garrido[1], Françoise Goirand[1†], Philippe Bonniaud[1,3,4 †‡]

- 1 INSERM U1231, Faculty of Medicine and Pharmacy, University of Bourgogne-Franche Comté, F-21000 Dijon, France
- 2 Division of Pulmonary Sciences and Critical Care Medicine, Department of Medicine, University of Colorado Denver, Aurora, CO, USA
- 3 Department of Pulmonary Medicine and Intensive Care Unit, University Hospital, Bourgogne-Franche Comté, F-21000 Dijon, France
- 4 Reference Center for Rare Lung Diseases, University Hospital, Bourgogne-Franche Comté, F-21000 Dijon, France
- 5 Cancer Center Georges François Leclerc, F-21000 Dijon, France
- 6 INSERM U1152, Faculty of Medicine, University of Bichat, F-75018 Paris, France
- 7 McMaster University, Hamilton, Canada
- †These authors codirected this work and contributed equally to this work.
- ‡Corresponding author.

Philippe Bonniaud, MD, PhD,
Department of Pulmonary Medicine and Intensive Care Unit, University Hospital, 21079 Dijon, France
tel : +33 3 80 29 32 63
e-mail : philippe.bonniaud@chu-dijon.fr

Author contributions: P-M.B, F.G., P.B. designed the study. P-M.B, O.B., G.B., P-S.B., L.D., G.M, L.P., A.V., M.S. and A.M. performed the experiments and data analyses. O.D. supervised the mouse breeding. MK provided adenoviruses. P-M.B. prepared the manuscript. B.C., M.K. and C.G. brought important intellectual content. O.B., P-S.B., F.G. and P.B. provided critical revision of the manuscript. All authors have read, reviewed and approved the final submitted manuscript and agree to take public responsibility for it.

Funding: This work received funding from the Agence Nationale de la Recherche (ANR SHOT-IPF). P-M.B. is supported by the "Fonds de Recherche en Santé Respiratoire" Appel d'offres Formation par la Recherche 2018 / Société de Pneumologie de Langue Française –SPLF-. O.B. was supported by the French "Investissements d'Avenir" program, project ISITE-BFC (contract ANR-15-IDEX-0003). O.B. has received funding from the European Respiratory Society and the European Union's H2020 research and innovation programme under the Marie Sklodowska-Curie grant agreement No 713406. The CG. team has the "label d'excellence" from La Ligue National Contre le Cancer and L'Association pour la "Recherche sur le Cancer" and belongs to the LabEx LipSTIC and GR-Ex.

Competing financial interests: The authors declare no competing financial interests.

Take home message: Our work demonstrates that TRIM33 has a protective role against fibrogenesis. TRIM33 inhibits the TGF-β1 pathway through a direct association with HSPB5 which impairs its activity. We believe that the interactions between TRIM33, SMAD4 and HSPB5 may represent a key target to prevent the progression of pulmonary fibrosis.

Abstract

Rationale: Idiopathic pulmonary fibrosis (IPF) is a devastating disease characterized by myofibroblast proliferation and abnormal extracellular matrix (ECM) accumulation in the lungs. Transforming-growth-factor (TGF)-β1 initiates key profibrotic signaling involving the SMADs pathway and the small heat shock protein αB-crystallin (HSPB5). TRIpartite Motif-containing 33 (TRIM33) has been reported to negatively regulate TGF-β/SMADs signaling but its role in fibrogenesis remains unknown.

Objectives: To elucidate the role of TRIM33 in IPF.

Methods: TRIM33 expression was assessed in the lungs of IPF patients and rodent fibrosis models. Bone Marrow-derived Macrophages (BMDM), primary lung fibroblasts and 3D-lung tissue slices were isolated from *Trim33*-floxed mice and cultured with TGF-β1 or bleomycin (BLM). *Trim33* expression was then suppressed by adenovirus–Cre recombinase (AdCre). Pulmonary fibrosis was evaluated in hematopoietic-specific *Trim33* knock-out (KO) mice and in *Trim33*-floxed mice that received AdCre and BLM intratracheally.

Results: TRIM33 was overexpressed in alveolar macrophages and fibroblasts in IPF patients and rodent fibrotic lungs. *Trim33* inhibition in BMDM increased TGF-β1 secretion upon BLM treatment. Hematopoietic-specific *Trim33*-KO sensitized mice to BLM-induced fibrosis. In primary lung fibroblasts and 3D-lung tissue slices, *Trim33*-deficiency increased TGF-β1-downstream gene expression. In mice, AdCre-*Trim33* inhibition worsened BLM-induced fibrosis. *In vitro*, HSPB5 was able to bind directly to TRIM33, thereby diminishing its protein level and TRIM33/SMAD4 interaction.

Conclusion: Our results demonstrate a key role of TRIM33 as a negative regulator of lung fibrosis. Since TRIM33 directly associates with HSPB5 which impairs its activity, inhibitors of TRIM33/HSPB5 interaction may be of interest in the treatment of IPF.

Introduction

Idiopathic pulmonary fibrosis (IPF) is a rare, chronic and progressive disease of the lung parenchyma of unknown origin, with a median survival of 3-5 years (1). With the exception of pirfenidone and nintedanib which exhibit moderate efficacy on disease progression; no pharmacologic treatment is currently available (2). IPF development associates abnormal alveolar repair with proliferation of activated fibroblasts named myofibroblasts, which leads to abnormal extracellular-matrix (ECM) accumulation and tissue remodeling. Transforming-growth-factor (TGF)-β1 is a key profibrotic growth factor, and the adenoviral vector-mediated gene transfer of active TGF-β1 (AdTGF-β1) in rodent lungs leads to progressive and severe fibrosis (3). TGF-β1 is responsible for fibroblast activation into myofibroblasts. Mechanistically, TGF-β1 classically signals via the SMADs proteins, a crucial pathway in fibrogenesis (4).

We previously demonstrated that the small heat shock protein (HSP) B5 (also termed αB-crystallin) is overexpressed in human IPF lungs. HSPB5 interferes with SMAD4 localization by inhibiting its export from the nucleus. At the molecular level, HSPB5 hampers SMAD4 ubiquitination and, consequently, Smad4 accumulates in the nucleus and promotes TGF-β1 signaling and fibrogenesis (5). TRIM33 is an E3-ubiquitin-ligase responsible for SMAD4 ubiquitination, inducing its export from the nucleus and therefore inhibiting SMADs transcriptional activity (6). TRIM33 is involved in several processes, such as embryogenesis, hematopoiesis and tumorigenesis (6-8). Specifically, TRIM33 is involved in the turnover of TGF-β receptor I (8) and in the innate immune response by regulating a subset of genes, including TGF-β1 or interferon-β in macrophages (9, 10). Anti-TRIM33 antibodies are elevated in humans with myositis, a set of diseases with increased prevalence of cancer and

interstitial lung disease (ILD) (11). However, the impact of TRIM33 in lung fibrosis and IPF remains unstudied.

In the current study, we demonstrate for the first time that TRIM33 is overexpressed in the lungs of IPF patients and has a protective effect against pulmonary fibrosis *in vivo*. In addition, we highlight a mechanism by which HSPB5 interferes with the anti-fibrotic properties of TRIM33, paving the way for the development of novel therapeutic strategies targeting the interaction between HSPB5 and TRIM33.

Materials and methods

Human tissue samples

Lung tissue samples (n = 5) were obtained by open lung biopsy (INSERM U700, Paris). IPF was diagnosed according to the American Thoracic Society/European Respiratory Society consensus criteria (12), including clinical, radiographic, and characteristic histopathologic features. Control non-IPF lung tissue samples were obtained from smokers who underwent thoracic surgery for localized primary lung carcinoma (n= 5). The local ethics committee (Comité de Protection des Personnes, Ile de France 1) approved the study, and patients provided informed consent before lung surgery.

Human microarray data

GSE110147 was performed and analyzed by Cecchini *et al*. (13) and GSE49072 was performed and analyzed by Shi *et al. (14).*

Animal procedures

SV129 Wild-Type (WT) mice (Charles River, Saint Germain-sur-l'Arbresle, France) and SV129 Knock-Out (KO) mice for the HSPB5 gene were housed in pathogen-free conditions. We generated mice selectively deficient for TRIM33 by breeding floxed *Trim33* mice with cFes-Cre transgenic mice. *Trim33*$^{f/f}$-Cre^{cFes} (hs*Trim33*$^{-/-}$) mice thus corresponded to hematopoietic-tissue-restricted KO mice, as previously described (15). Mouse food and water were provided *ad libitum*. The animals were treated according to the guidelines of the "Ministère de l'Enseignement Supérieur et de la Recherche" (Paris, France). All experiments were approved by the "Comité d'Ethique de l'Expérimentation Animale du grand campus Dijon" (Bourgogne, France). Intratracheal instillation of BLM at 1.5 mg/kg (Santa Cruz biotechnology, Dallas, USA) was performed as previously described (16). AdTGF-β1 (5.10^8 PFU/mouse) and AdCre (5.10^8 PFU/mouse) were instilled following the same protocol. BLM and adenovirus were diluted in 0.9% NaCl. Mice were euthanized by abdominal aortic bleeding at day 21 after administration. Bronchoalveolar lavage fluid (BALF) was gathered as previously described (17).

Collagen quantification

Histomorphometric assay - The amount of collagen in paraffin-embedded tissue sections was quantified by staining with Picrosirius Red as previously described (18, 19).

Colorimetric assay - The sircol assay was performed on lung left lobe extracts using the "Sircol kit" (Biocolor Ltd., Carrickfergus, UK) and following the manufacturer's recommendations.

Precision Cut Lung Slice preparation

3D-lung tissue slices were generated as previously described (20) and cultured for 72h in DMEM + 10% serum, 1% L-glutamine and 1% penicillin/streptomycin. 3 slices were pooled for each mRNA extraction.

Statistical analysis

Comparisons between different groups were performed using the non-parametric Mann-Whitney test and Prism 6 software (Graphpad, San Diego, CA ,USA). P values below 0.05 were considered statistically significant. All results are representative of at least 3 different experiments.

Results

TRIM33 is upregulated during pulmonary fibrosis

Histological examination of IPF lungs showed overexpression of TRIM33 as compared to non-IPF control lungs, in which TRIM33 was barely detectable (Figure 1A). TRIM33 was overexpressed preferentially in myofibroblasts expressing smooth muscle actin (α-SMA) and in macrophages expressing Macrosialin (CD68). TRIM33 overexpression could also be observed in ATII cells expressing pulmonary surfactant-associated protein C (SP-C, Figure 1B). Analysis of publicly available microarray data (GSE110147) showed that *TRIM33* mRNA level was upregulated in total lung tissue from IPF patients compared to control lung tissue (Figure 1C, left panel) but also specifically in alveolar macrophages from IPF patients (GSE49072, Figure 1C right panel). The analysis of our patient cohort confirmed the increase of *TRIM33* expression in the whole lung tissue of IPF patients compared to control tissue (Supplemental Figure 1A).

Similarly to human, TRIM33 was upregulated in fibrotic areas of mice receiving repeated intravenous (IV) injections of bleomycin (BLM, Figure 2A). This increase was confirmed by immunoblotting and rt-qPCR (Figure 2B-C). Trim33 upregulation was also observed in fibrotic areas in other models of lung and pleural fibrosis, such as in mice receiving a single intra-tracheal (it) instillation of BLM, or in rats and mice receiving an intrapleural injection of adenovirus encoding for TGF-β1 (AdTGF) compared to control rodents (Supplemental Figure 2A). In the BLM model, Trim33 was expressed in fibroblasts (Vimentin) and macrophages (CD68) (Supplemental Figure 2B).

Trim33 inhibition impairs TGF-β1 secretion in macrophages

As *TRIM33* is overexpressed in alveolar macrophages of IPF patients (Figure 1B-C), we investigated the effects of TRIM33 on bone marrow derived macrophages (BMDM). BMDM isolated from *Trim33*-floxed (*Trim33*$^{f/f}$) mice were depleted for *Trim33* by *ex vivo* exposure to an adenovirus encoding the Cre-recombinase (AdCre, Figure 3A). *Trim33* depletion was confirmed using qPCR (Supplemental Figure 3A). BLM stimulation of BMDM expressing TRIM33 lead to an increase in TGF-β1, TNF-α and IL-6 production (Figure 3B), with no impact on cellular viability (Supplemental Figure 3C). The depletion of *Trim33* did not affect the level of TGF-β1 without stimulation while it resulted in a 3-fold increase in TGF-β1 secretion upon BLM stimulation. In parallel, we did not observe any significant difference in Tgfb1 gene expression (Supplemental Figure 3B), in secretion of pro-inflammatory cytokines (TNF-α and Il-6, Figure 3B) or other cytokines (Supplemental Figure 3D) between BMDM expressing TRIM33 (AdDL) and BMDM depleted for TRIM33 (AdCre), both at basal level or upon BLM exposure. Next, we investigated the functional effect of *Trim33* deficiency in the crosstalk between macrophages and lung fibroblasts (Figure 3C). Conditioned media were collected from

BMDM cultured in four distinct conditions: 1/ Unstimulated BMDM expressing *Trim33* (AdDL NT), 2/ BMDM expressing *Trim33* stimulated with BLM (AdDL BLM), 3/ unstimulated BMDM depleted for *Trim33* (AdCre NT) and 4/ BMDM depleted for *Trim33* stimulated with BLM (AdCre BLM). The expression of mesenchymal markers was then investigated in mouse primary pulmonary fibroblasts incubated with these conditioned media. Conditioned media from unstimulated BMDM, expressing *Trim33* or not (AdDL NT and AdCre NT), had no impact on the expression of mesenchymal markers in fibroblasts (Figure 3C). However, conditioned media from BLM-stimulated BMDM expressing *Trim33* (AdDL BLM) induced an increase in mesenchymal markers which was further enhanced when fibroblasts were stimulated by conditioned media from BLM-stimulated BMDM depleted for *Trim33* (comparison media BMDM AdDL BLM vs. BMDM AdCre BLM; Actin Alpha 2, Smooth Muscle *(Acta2)*: 1.87-fold increase, Serpin Family E Member 1 (*Serpine1)*: 1.46-fold increase, Lymphoid enhancer-binding factor 1 (*Lef1)* : 1.66-fold increase and Vimentin (*Vim)*: 1.2-fold increase. Figure 3C). Altogether, these results suggest that although *Trim33* deficiency has no impact on TGF-β1 secretion at the basal level, yet it can promote the production of active profibrotic factors upon BLM stimulation, which in turn activates lung fibroblasts.

Hs*Trim33*$^{-/-}$ mice are more sensitive to bleomycin-induced pulmonary fibrosis

To confirm the *in vivo* significance of TRIM33 in immune cells during pulmonary fibrosis development, we used mice with cFes-driven Cre to generate conditional *Trim33* KO mice resulting in *Trim33* depletion specifically in the hematopoietic system: *Trim33*$^{f/f}$-Cre^{cFes} mice (hs*Trim33*$^{-/-}$ mice, Figure 4A) (15). Following BLM challenge, hs*Trim33*$^{-/-}$ mice developed more severe fibrosis compared to control mice (*Trim33*$^{f/f}$ mice), characterized by worsened pulmonary alveolar structure remodeling and increased collagen accumulation throughout

the lungs (Figure 4B). Picrosirius red staining of lung sections showed a 1.7-fold increase in collagen lung content in hs*Trim33*$^{-/-}$ mice compared to a 1.4-fold increase in control mice (Supplemental Figure 4A). This result was confirmed by a Sircol assay in which we found that BLM induced a significant increase in collagen content in hs*Trim33*$^{-/-}$ mouse lungs compared to control lungs (Figure 4C). In lung tissues, the increase in *Acta2* mRNA level induced by BLM was significantly higher in hs*Trim33*$^{-/-}$ mice compared to control mice (supplemental Figure 4B). Similar findings were observed after repetitive systemic intravenous BLM exposure (Supplemental Figure 5A-B-C).

Confirming our *in vitro* results, TGF-β1 level was significantly increased in the bronchoalveolar lavage fluid (BALF) from hs*Trim33*$^{-/-}$ mice compared to control WT mice exposed to BLM (2-fold increase). In parallel, there was no difference in TNF-α and IL-6 protein level in BALF from hs*Trim33*$^{-/-}$ versus control mice after BLM exposure (Figure 4D).

Altogether, these results suggest that TRIM33 significantly represses the establishment of a pro-fibrotic microenvironment, specifically by inhibiting the production of active TGF-β1 by immune cells, including macrophages.

Trim33 depletion promotes TGF-β1-downstream signaling pathways ex vivo

As TRIM33 was also overexpressed in fibroblasts from IPF patients (Figure 1), we investigated the effects of TRIM33 expression in primary pulmonary fibroblasts. We isolated primary pulmonary fibroblasts from *Trim33*$^{f/f}$ mice and depleted *Trim33* gene by infection with AdCre (or AdDL as control, Figure 5A). The loss of TRIM33 expression was confirmed by western blot (Figure 5B). Treatment of control (AdDL) fibroblasts with recombinant TGF-β1 (rTGF-β1) induced an upregulation of the SMADs pathway downstream gene mRNAs (*Acta2*, *Serpine1*, *Lef1*, Twist Family BHLH Transcription Factor 1 *(Twist1)*, Figure 5C). Interestingly,

the upregulation of those genes was further increased in *Trim33*-depleted fibroblasts (AdCre) compared to AdDL fibroblasts (respectively 2.98-fold increase for *Acta2*, 2.05 for *Serpine1*, 3.2 for *Lef1* and 1.8 for *Twist1*, Figure 5C). These results were confirmed using 3D-lung tissue slices generated from *Trim33*$^{f/f}$ mice and treated with AdCre (Figure 5D). *Trim33* depletion was confirmed by qPCR (Figure 5D) and we showed that this depletion induced, upon TGF-β1, a significant increase in *Acta2*, *Serpine1* and Collagen Type I Alpha 1 Chain (*Col1a1)* mRNA (respectively 1.9-fold increase expression for *Acta2*, 1.3 for *Serpine1* and 1.54 for *Col1a1,* Figure 5D).

Therefore, TRIM33 appears to negatively control TGF-β1-downstream signaling by blocking over-activation of the TGF-β1 pathway in fibrotic conditions.

Trim33 inhibition in the lungs worsens BLM-induced fibrosis in mice

To confirm the *in vivo* significance of *Trim33* expression in the lungs, we depleted *Trim33* in *Trim33*$^{f/f}$ mouse lungs by i.t. administration of AdCre (Figure 6A).

We observed in our model that 29.7% of the lung cells underwent recombination 48h after AdCre i.t. instillation, as measured using flow cytometry (Supplemental Figure 6A). AdCre instillation was able to induce recombination mostly in CD326 (Epithelial cell adhesion molecule) positive cells (epithelial) but also in ER-TR7 positive cells (fibroblasts) and in some CD68 positive cells (macrophages) (Supplemental Figure 6B-C). Three days after AdCre exposure, mice were challenged with BLM and fibrosis was assessed at 21 days post-BLM. AdCre-mediated *Trim33* depletion in mice resulted in more severe fibrosis after BLM intra-tracheal challenge, compared to the AdDL mice expressing normal levels of TRIM33 (Figure 6B-C, Supplemental Figure 7A). The up-regulation of fibrosis-related genes induced by BLM at the mRNA level was significantly higher in AdCre mice compared to AdDL mice

(respectively 1.64-fold increase for *Col1a1*, 1.41 for *Serpine1* and 1.3-fold for *Twist1*, Supplemental Figure 7A). Up-regulation of fibrosis-related markers was also found at the protein level for Plasminogen activator inhibitor 1 (PAI-1), Type I collagen as well as for HSPB5 (Figure 6D). As expected, mice treated with AdDL showed an increase in TRIM33 protein level upon BLM, whereas mice treated with AdCre did not (Figure 6D). Interestingly, whereas depletion of *Trim33* potentiated fibrogenesis marker induction, in non-fibrotic conditions it did not appear to have any effect on collagen accumulation, mesenchymal differentiation nor on the immune cell profile of the BALF (Supplemental Figure 7A-B).

TRIM33 activity and protein level are impaired by HSPB5 overexpression

TRIM33 and HSPB5 are described as key regulators of the TGF-β1/SMADs pathway. HSPB5 was up-regulated following AdCre-mediated *Trim33* depletion, suggesting a mechanistic regulation between both proteins. In the pulmonary tissue of *Hspb5* deficient mice (*Hspb5-KO,* Supplemental Figure 8A), TRIM33 protein level was increased compared with WT mice (Figure 7A). This difference was further amplified following BLM challenge. At the same time, the depletion of *Hspb5* induced no change in *Trim33* mRNA level in total lung tissue (Figure 7B). Similar results were found using primary pulmonary fibroblasts from *Hspb5*-KO mice treated *ex vivo* with TGF-β1 (Supplemental Figure 8B). On the other hand, *HSPB5* overexpression in human alveolar epithelial A549 cells induced a decrease in TRIM33 protein level (Figure 7C), again without interfering with its mRNA level (Figure 7D). Our data suggest that in parallel to the induction of its expression after *TRIM33* depletion, HSPB5 negatively regulates TRIM33 protein level in a post-translational manner.

Next, we further investigated the protein-protein interaction between HSPB5 and TRIM33. Bio-Layer Interferometry experiments using recombinant purified proteins showed that

TRIM33 was able to bind directly to both HSPB5 with a Kd of $2.91x10^{-9}$ M and SMAD4 with a Kd of $1.28x10^{-9}$ M (Supplemental Figure 8C-D). Furthermore, by FLIM-FRET analysis, we showed that HSPB5 overexpression decreased SMAD4-TRIM33 interaction (Supplemental Figure 8E). In line with these results and the previously described inhibitory role of HSPB5 on TRIM33 activity, we demonstrated that HSPB5 was able to reduce the SUMOylation of TRIM33, which is essential for its E3 ubiquitin-ligase activity on SMAD4 (Figure 7E).

Altogether, these results demonstrate a feedback loop between HSPB5 and TRIM33, respectively positive and negative regulators of the SMADs pathway. We show that TRIM33 level is impaired upon HSPB5 overexpression. Further, we uncover that HSPB5 promotes TRIM33 SUMOylation and thus inhibits its binding to SMAD4, leading to enhanced TGF-β1 signaling.

Discussion

TRIM33 is an E3-ubiquitin-ligase known as a negative regulator of TGF-β1 signaling, one of the most potent profibrotic signal, through SMAD4 ubiquitination and turnover of TGF-β receptors (6, 8). We show that TRIM33 is up-regulated in both IPF patients and rodent models of lung fibrosis. *Trim33* depletion *in vitro* and *in vivo* causes an exacerbation of fibroblast activation, collagen deposition and pro-fibrogenic factors secretion under profibrotic conditions (i.e. on BLM or TGF-β1 exposure) suggesting a protective role of TRIM33 in lung fibrosis. Therefore, the upregulation of TRIM33 may be viewed as a failing attempt to prevent fibrosis progression in IPF and models of lung fibrosis. TRIM33 inhibitory properties on TGF-β1 signaling might be due to an insufficient level of expression or an intrinsic inhibition of its activity. The present works sheds light on this regulation.

Analysis of publically available datasets demonstrates an upregulation of TRIM33 in IPF lungs. Yet, we hypothesize that the level of upregulation compared to control lungs remains moderate and insufficient to exert its anti-fibrotic action. Nevertheless, datasets only recapitulate mRNA expression which may not be representative of the real level of TRIM33 neither at the protein level nor in term of activity in the IPF lungs. Our data show that TRIM33 protein is markedly upregulated mainly in myofibroblasts, macrophages and also alveolar epithelial cells suggesting that TRIM33 may encounter post-translational regulations which prevent its anti-fibrotic functions. Our team previously demonstrated that HSPB5 up-regulation in IPF induced a decrease in the interaction between TRIM33 and SMAD4, hampering the ubiquitination and the nuclear export of the latter (5). In this context, HSPB5 may serve as a physiologic inhibitor of TRIM33 negative control on TGF-β1 signaling. Further, we show that TRIM33 is able to bind to both HSPB5 and SMAD4 directly. Within this complex, HSPB5 appears to reduce the level of SUMOylation of TRIM33 therefore reducing its binding ability to ubiquitinate SMAD4 and resulting in an exacerbation of the pro-fibrotic TGF-β1 signaling. We believe that the inhibition of the interaction between TRIM33 and HSPB5 may be able to restore TRIM33 repressor effects on the TGF-β1 pathway and may be of interest for the treatment of IPF.

Among lung cells, we demonstrate that alveolar macrophages are one of the main cell type expressing TRIM33 in human and rodent lung fibrosis. While the role of inflammation in pulmonary fibrosis remains controversial (21) and despite the lack of efficacy of anti-inflammatory therapies on IPF progression, unbiased approaches unraveled a significant immune component in IPF and alveolar macrophages appear to be critical for the development of lung fibrosis (22, 23). Macrophage activation is heavily involved in fibrogenesis regulation in various tissues including the liver, kidney and the lungs (24) mainly

through the secretion of TNF-α, Il-6 and most importantly TGF-β1 (25), the latter being able to modulate fibroblast proliferation and extra-cellular matrix production (26). As macrophages are able to produce a variety of pro-fibrotic signals, we hypothesized that TRIM33 may have a key role in controlling macrophages secretory profile in a fibrotic context. While TRIM33 has been demonstrated to play a role in the inflammatory response in BMDM (27), we show here, in fibrotic conditions, that *Trim33*-deficiency induces an increase in active TGF-β1 secretion by BMDM. This depletion does not modify the secretion of pro-inflammatory cytokines TNF-α and IL-6, demonstrating a rather specific mechanism towards the TGF-β1 pathway. Remarkably, we demonstrate that *Trim33* deficiency does not interfere with *Tgfb1* gene expression. TGF-β1 is primarily produced in an inactive form which requires to be processed inside and outside the cell in order to be secreted and activated. As a consequence TGF-β1 activity is mainly regulated by post-translational modifications. Therefore, our data suggest that *Trim33* depletion may interfere indirectly with the mechanisms involved in TGF- β1 maturation rather than with the *Tgfb1* gene expression.

Myofibroblasts are of major importance in pulmonary fibrosis, as they are the main secretor of ECM. They can originate from various cell types, including resident fibroblasts, fibrocytes, and differentiated fibroblasts via cellular reprogramming of epithelial cells (28). TRIM33 has been demonstrated to be involved in mesenchymal differentiation in the context of oncology. For instance, *TRIM33* depletion in epithelial cells has been linked to enhanced mesenchymal differentiation in several cancer models including non-small-cell lung cancer (29), NMuMG mammary epithelial cells (30) and renal cell carcinoma (31). In lung fibrosis conditions, we demonstrate that *Trim33* depletion, in primary pulmonary fibroblasts, as well as in *ex vivo* lung tissue, promotes mesenchymal differentiation. In addition, depletion of *Trim33* in the lungs by intratracheal administration of AdCre increased sensitivity to

bleomycin-induced fibrosis with an increase in ECM deposition. These results may suggest a crucial role of TRIM33 in the activation of mesenchymal differentiation leading to an increase in the amount of myofibroblasts and subsequent exaggerated ECM deposition.

It is noteworthy that TRIM33 antibodies are found in the serum of patients in pathological conditions such as polymyositis and dermatopolymyositis. These diseases are associated with cancer but also with interstitial lung diseases (ILD) (11). These ILD present as non-specific interstitial pneumonia or with a pattern of usual interstitial pneumonia, as observed in IPF (32). Although the pathogenic role of TRIM33 antibodies is beyond the scope of the current work, we believe that they have to be further explored to better understand their protective or aggravating role in IPF.

Thus, we hypothesize that TRIM33 is induced in pro-fibrotic conditions as part of a negative feedback loop to slow-down an exacerbated activation of TGF-β1 signaling. However, in several pathological conditions, such as IPF, the negative control exerted by TRIM33 is swallowed due to either an inefficient up-regulation or due to an inhibition by other up-regulated proteins in fibrotic conditions, such as HSPB5.

Conclusion

Our work demonstrates that TRIM33 is overexpressed in the lung during fibrotic conditions and we show that TRIM33 has a protective role against fibrogenesis by inhibiting the TGF-β1 pathway independently of inflammation. We believe that TRIM33 expression may represent an attempt to resolve the fibrotic process, which is overwhelmed during IPF. We believe that the complex interactions between TRIM33, SMAD4 and HSPB5 may represent key targets to

prevent progression of fibrosis in case of induced lung fibrosis as in iatrogenic diseases or in IPF.

Acknowledgments: We thank V. Saint-Giorgio, the Cellimap core facility for the microscopy and immunohistochemistry, Dr P. Winckler, from the Dimacell imaging facility, UMR PAM, Université de Bourgogne/Agrosup Dijon, France for technical assistance in the FLIM-FRET experiments. We are grateful to Dr. L. Delva for providing the cFes-Cre and the floxed-*Trim33* mice. Illustrations were adapted from Smart Servier Medical Art.

Reference

1. Raghu G, Rochwerg B, Zhang Y, Garcia CAC, Azuma A, Behr J, Brozek JL, Collard HR, Cunningham W, Homma S. An official ats/ers/jrs/alat clinical practice guideline: Treatment of idiopathic pulmonary fibrosis. An update of the 2011 clinical practice guideline. *American journal of respiratory and critical care medicine* 2015;192:e3-e19.
2. Martinez FJ, Collard HR, Pardo A, Raghu G, Richeldi L, Selman M, Swigris JJ, Taniguchi H, Wells AU. Idiopathic pulmonary fibrosis. *Nature Reviews Disease Primers* 2017;3:17074.
3. Bonniaud P, Margetts PJ, Kolb M, Haberberger T, Kelly M, Robertson J, Gauldie J. Adenoviral gene transfer of connective tissue growth factor in the lung induces transient fibrosis. *American journal of respiratory and critical care medicine* 2003;168:770-778.
4. Bonniaud P, Margetts PJ, Ask K, Flanders K, Gauldie J, Kolb M. Tgf-β and smad3 signaling link inflammation to chronic fibrogenesis. *The Journal of Immunology* 2005;175:5390-5395.
5. Bellaye P-S, Wettstein G, Burgy O, Besnard V, Joannes A, Colas J, Causse S, Marchal-Somme J, Fabre A, Crestani B, Kolb M, Gauldie J, Camus P, Garrido C, Bonniaud P. The small heat-shock proteinαb-crystallin is essential for the nuclear localization of smad4: Impact on pulmonary fibrosis. *The Journal of Pathology* 2014;232:458-472.
6. Dupont S, Mamidi A, Cordenonsi M, Montagner M, Zacchigna L, Adorno M, Martello G, Stinchfield MJ, Soligo S, Morsut L, Inui M, Moro S, Modena N, Argenton F, Newfeld SJ, Piccolo S. Fam/usp9x, a deubiquitinating enzyme essential for tgfβ signaling, controls smad4 monoubiquitination. *Cell* 2009;136:123-135.
7. Morsut L, Yan KP, Enzo E, Aragona M, Soligo SM, Wendling O, Mark M, Khetchoumian K, Bressan G, Chambon P, Dupont S, Losson R, Piccolo S. Negative control of smad activity by ectodermin/tif1 patterns the mammalian embryo. *Development* 2010;137:2571-2578.
8. Quere R, Saint-Paul L, Carmignac V, Martin RZ, Chretien ML, Largeot A, Hammann A, Pais de Barros JP, Bastie JN, Delva L. Tif1 regulates the tgf- 1 receptor and promotes physiological aging of hematopoietic stem cells. *Proceedings of the National Academy of Sciences* 2014;111:10592-10597.
9. Gallouet A-S, Ferri F, Petit V, Parcelier A, Lewandowski D, Gault N, Barroca V, Le Gras S, Soler E, Grosveld F. Macrophage production and activation are dependent on trim33. *Oncotarget* 2017;8:5111.
10. Ferri F, Parcelier A, Petit V, Gallouet A-S, Lewandowski D, Dalloz M, Van Den Heuvel A, Kolovos P, Soler E, Squadrito ML. Trim33 switches off ifnb1 gene transcription during the late phase of macrophage activation. *Nature communications* 2015;6:8900.

11. Hozumi H, Enomoto N, Kono M, Fujisawa T, Inui N, Nakamura Y, Sumikawa H, Johkoh T, Nakashima R, Imura Y. Prognostic significance of anti-aminoacyl-trna synthetase antibodies in polymyositis/dermatomyositis-associated interstitial lung disease: A retrospective case control study. *PLoS One* 2015;10:e0120313.
12. Raghu G, Collard HR, Egan JJ, Martinez FJ, Behr J, Brown KK, Colby TV, Cordier JF, Flaherty KR, Lasky JA, Lynch DA, Ryu JH, Swigris JJ, Wells AU, Ancochea J, Bouros D, Carvalho C, Costabel U, Ebina M, Hansell DM, Johkoh T, Kim DS, King TE, Jr., Kondoh Y, Myers J, Muller NL, Nicholson AG, Richeldi L, Selman M, Dudden RF, Griss BS, Protzko SL, Schunemann HJ, Fibrosis AEJACoIP. An official ats/ers/jrs/alat statement: Idiopathic pulmonary fibrosis: Evidence-based guidelines for diagnosis and management. *American journal of respiratory and critical care medicine* 2011;183:788-824.
13. Cecchini MJ, Hosein K, Howlett CJ, Joseph M, Mura M. Comprehensive gene expression profiling identifies distinct and overlapping transcriptional profiles in non-specific interstitial pneumonia and idiopathic pulmonary fibrosis. *Respiratory research* 2018;19:153.
14. Shi Y, Gochuico BR, Yu G, Tang X, Osorio JC, Fernandez IE, Risquez CF, Patel AS, Shi Y, Wathelet MG. Syndecan-2 exerts antifibrotic effects by promoting caveolin-1–mediated transforming growth factor-β receptor i internalization and inhibiting transforming growth factor-β1 signaling. *American journal of respiratory and critical care medicine* 2013;188:831-841.
15. Chrétien M-L, Legouge C, Martin RZ, Hammann A, Trad M, Aucagne R, Largeot A, Bastie J-N, Delva L, Quéré R. Trim33/tif1γ is involved in late stages of granulomonopoiesis in mice. *Experimental hematology* 2016;44:727-739. e726.
16. Decologne N, Wettstein G, Kolb M, Margetts P, Garrido C, Camus P, Bonniaud P. Bleomycin induces pleural and subpleural fibrosis in the presence of carbon particles. *The European respiratory journal* 2010;35:176-185.
17. Bonniaud P, Margetts PJ, Ask K, Flanders K, Gauldie J, Kolb M. Tgf-beta and smad3 signaling link inflammation to chronic fibrogenesis. *Journal of immunology* 2005;175:5390-5395.
18. Blobe GC, Schiemann WP, Lodish HF. Role of transforming growth factor beta in human disease. *The New England journal of medicine* 2000;342:1350-1358.
19. Decologne N, Kolb M, Margetts PJ, Menetrier F, Artur Y, Garrido C, Gauldie J, Camus P, Bonniaud P. Tgf-beta1 induces progressive pleural scarring and subpleural fibrosis. *Journal of immunology* 2007;179:6043-6051.
20. Uhl FE, Vierkotten S, Wagner DE, Burgstaller G, Costa R, Koch I, Lindner M, Meiners S, Eickelberg O, Königshoff M. Preclinical validation and imaging of wnt-induced repair in human 3d lung tissue cultures. *European Respiratory Journal* 2015;46:1150-1166.
21. Strieter RM. Inflammatory mechanisms are not a minor component of the pathogenesis of idiopathic pulmonary fibrosis. *American journal of respiratory and critical care medicine* 2002;165:1206-1207.
22. Schiller HB, Mayr CH, Leuschner G, Strunz M, Staab-Weijnitz C, Preisendörfer S, Eckes B, Moinzadeh P, Krieg T, Schwartz DA. Deep proteome profiling reveals common prevalence of mzb1-positive plasma b cells in human lung and skin fibrosis. *American Journal of Respiratory and Critical Care Medicine* 2017;196:1298-1310.
23. Misharin AV, Morales-Nebreda L, Reyfman PA, Cuda CM, Walter JM, McQuattie-Pimentel AC, Chen C-I, Anekalla KR, Joshi N, Williams KJ. Monocyte-derived alveolar macrophages drive lung fibrosis and persist in the lung over the life span. *Journal of Experimental Medicine* 2017;214:2387-2404.
24. Song E, Ouyang N, Hörbelt M, Antus B, Wang M, Exton MS. Influence of alternatively and classically activated macrophages on fibrogenic activities of human fibroblasts. *Cellular immunology* 2000;204:19-28.
25. Della Latta V, Cecchettini A, Del Ry S, Morales MA. Bleomycin in the setting of lung fibrosis induction: From biological mechanisms to counteractions. *Pharmacological research* 2015;97:122-130.

26. Bonner JC, Osornio-Vargas AR, Badgett A, Brody AR. Differential proliferation of rat lung fibroblasts induced by the platelet-derived growth factor-aa,-ab, and-bb isoforms secreted by rat alveolar macrophages. *American Journal of Respiratory Cell and Molecular Biology* 1991;5:539-547.
27. Tanaka S, Jiang Y, Martinez GJ, Tanaka K, Yan X, Kurosaki T, Kaartinen V, Feng X-H, Tian Q, Wang X, Dong C. Trim33 mediates the proinflammatory function of th17 cells. *The Journal of Experimental Medicine* 2018:jem.20170779.
28. Xie T, Wang Y, Deng N, Huang G, Taghavifar F, Geng Y, Liu N, Kulur V, Yao C, Chen P. Single-cell deconvolution of fibroblast heterogeneity in mouse pulmonary fibrosis. *Cell reports* 2018;22:3625-3640.
29. Wang L, Yang H, Lei Z, Zhao J, Chen Y, Chen P, Li C, Zeng Y, Liu Z, Liu X. Repression of tif1γ by sox2 promotes tgf-β-induced epithelial–mesenchymal transition in non-small-cell lung cancer. *Oncogene* 2016;35:867.
30. Ikeuchi Y, Dadakhujaev S, Chandhoke AS, Huynh MA, Oldenborg A, Ikeuchi M, Deng L, Bennett EJ, Harper JW, Bonni A, Bonni S. Tif1γ protein regulates epithelial-mesenchymal transition by operating as a small ubiquitin-like modifier (sumo) e3 ligase for the transcriptional regulator snon1. *Journal of Biological Chemistry* 2014;289:25067-25078.
31. Jingushi K, Ueda Y, Kitae K, Hase H, Egawa H, Ohshio I, Kawakami R, Kashiwagi Y, Tsukada Y, Kobayashi T. Mir-629 targets trim33 to promote tgfβ/smad signaling and metastatic phenotypes in ccrcc. *Molecular Cancer Research* 2014.
32. Mugii N, Hasegawa M, Matsushita T, Hamaguchi Y, Oohata S, Okita H, Yahata T, Someya F, Inoue K, Murono S. Oropharyngeal dysphagia in dermatomyositis: Associations with clinical and laboratory features including autoantibodies. *PLoS One* 2016;11:e0154746.

Figure 1: TRIM33 is up-regulated in lungs of IPF patients. (A) TRIM33 immunostaining in lungs of control (n = 4) or IPF patients (n= 4), scale bar: 100 µm. (B) TRIM33 (brown), a-SMA (green), CD68 (green), and SP-C (red) immunostaining in control lungs (n= 3) or IPF lungs (n= 3), scale bar: 100 µm. (C) Left Panel : Analysis of publicly available microarray data (accession number GSE110147) from lung samples from 22 IPF patients undergoing lung transplantation and 11 normal lung tissues flanking lung cancer resections. Results are expressed as median with interquartile range; ****P = 0.0001, unpaired t test with Welch's correction. Right panel: Analysis of publicly available microarray data (accession number GSE49072) from alveolar macrophages isolated from 31 IPF patients and 61 normal volunteers or unaffected relatives. Results are expressed as median with interquartile range; ****P = 0.0001, unpaired t test with Welch's correction.

Figure 2: Trim33 is up-regulated during bleomycin-induced pulmonary fibrosis.(A) Representative images of TRIM33 immunostaining on lung sections from mice given either bleomycin or NaCl by intravenous injections (n=5), scale bar: 250 µm. (B) Western blot and (C) mRNA levels of Trim33 in mice given either BLM or NaCl by intravenous injection (n=4-5 per group). Results are expressed as median with interquartile range; *P = 0.05, non-parametric Mann-Whitney test. BLM : bleomycin

Figure 3: Trim33 inhibition impairs TGF-ß1 secretion in macrophages. (A) Cartoon showing the Cre-LoxP system used to deplete Trim33 in BMDM. (B) Mouse active TGF-ß1, TNF-a and IL-6 measured by ELISA in supernatant of BMDM from Trim33f/f mice exposed to AdDL or AdCre and either NaCl or bleomycin (48h, 5 mg/ml, n=3 each with 2 biological replicates). (C) mRNA levels of Acta2, Serpine1, Lef1 and Vim were analyzed by quantitative PCR in murine primary pulmonary fibroblasts treated with supernatant from BMDM exposed to AdDL or AdCre and either NaCl or BLM (48h, 5mg/ml, n=3 each with 3 biological replicates). Results are expressed as median with interquartile range; *P < 0.05, **P < 0.01, ***P < 0.001, non-parametric Mann-Whitney test. BLM : bleomycin.

Figure 4: hsTrim33-/- mice are more sensitive to bleomycin-induced pulmonary fibrosis. (A) Cartoon showing the Cre-LoxP system used to deplete Trim33 in hematopoietic lineage cells. (B) Representative histology of control mice (Trim33f/f) and hsTrim33-/- mice lungs 21 days after intratracheal injection of NaCl or bleomycin (1.5 mg/kg). Masson's trichrome staining (n= 6), scale bar: 250 µm. (C) Collagen quantification using a Sircol assay on the left-lung extract from control and hsTrim33-/- mice given either NaCl or bleomycin (at day 21). Results are expressed as median with interquartile range; *P < 0.05, **P < 0.01, non-parametric Mann-Whitney test; n= 4-9 per group. (D) Mouse Active TGF-ß1, TNF-a and IL-6 were measured by ELISA in BALF from control and hsTrim33-/- mice 21 days after intratracheal instillation of bleomycin or NaCl ; Results are expressed as median with interquartile range; *P < 0.05, **P < 0.01, non-parametric Mann-Whitney test ; n= 4-8 per group. BLM : bleomycin, n.s.; non significant.

Figure 5: Downregulation of Trim33 promotes TGF-ß1-downstream pathways. (A) Cartoon showing the Cre-LoxP system used to deplete Trim33 in primary lung fibroblasts. (B) TRIM33 expression was analyzed by western blot in pulmonary primary fibroblasts, generated from Trim33f/f mice, infected with AdDL or AdCre and then cultured with rTGF-ß1 (48h, 10ng/ml) (n=3). (C) mRNA levels of Acta2, Serpine1, Lef1 and Twist1 were analyzed by quantitative PCR of pulmonary primary fibroblasts, isolated from Trim33f/f mice, infected with AdDL or AdCre and then cultured with rTGF-ß1 (48h, 10ng/ml) (n=4 each with 2 biological replicates). Results are expressed as median with interquartile range; *P < 0.05, **P < 0.01 non-parametric Mann-Whitney test. (D) mRNA levels of Trim33, Acta2, Serpine1 and Col1a1 were analyzed by quantitative PCR on 3D-lung tissue slices generated from Trim33f/f mice, infected with AdDL or AdCre and then cultured with rTGF-

ß1 (48h, 10ng/ml) (n=3 each with 2 biological replicates). Results are expressed as median with interquartile range; *P < 0.05, **P < 0.01, non-parametric Mann- Whitney test.

Figure 6: Trim33 inhibition in the lungs worsens bleomycin-induced fibrosis in mice. (A) Cartoon showing the Cre-LoxP system used to deplete Trim33 in mouse lung. (B) Representative histology of Trim33f/f mouse lungs infected with AdDL or AdCre, then challenged 3 days later with intratracheal injection of NaCl or BLM (1.5 mg/kg). Representative images of Masson's trichrome collagen staining at day 21 after instillation (n= 6), scale bar 250 µm. (C) Collagen quantification (21 days after bleomycin treatment) using a Sircol assay on the left-lung from mice infected by AdDL or AdCre and given either NaCl or bleomycin. Results are expressed as median with interquartile range; *P < 0.05, **P < 0.01, non-parametric Mann-Whitney test; n= 5-8 per group. (D) Protein levels of TRIM33, PAI-1, HSPB5 and Type1 collagen were analyzed by Western Blot (left panel) in lungs from mice infected by AdDL or AdCre, 21 days after NaCl or bleomycin treatment. Densitometry (right panel) is expressed as median with interquartile range; *P < 0.05, **P < 0.01, non-parametric Mann-Whitney test. BLM: bleomycin.

Figure 7: TRIM33 activity and protein level are impaired by HSPB5 overexpression. (A) Protein level of TRIM33 in lungs from SV129 control mice (WT) or SV129 Hspb5-/- mice (Hspb5-KO). (B) mRNA levels of Trim33 analyzed by quantitative PCR in lungs from SV129 control mice or SV129 Hspb5-KO mice 21 days after bleomycin (BLM) treatment (n=4-8 per group). (C) Western blot and (D) mRNA level of TRIM33 in A549 cells transfected with a plasmid encoding HSPB5 (HSPB5) or the empty vector as control (Ctrl) (n=3). (E) Pull-down of SUMO-1-his in A549 cells after transfection with either TRIM33 and/or HSPB5 and/or SUMO-1, as indicated (n=3). The arrow head indicates a potential sumoylated form of TRIM33.

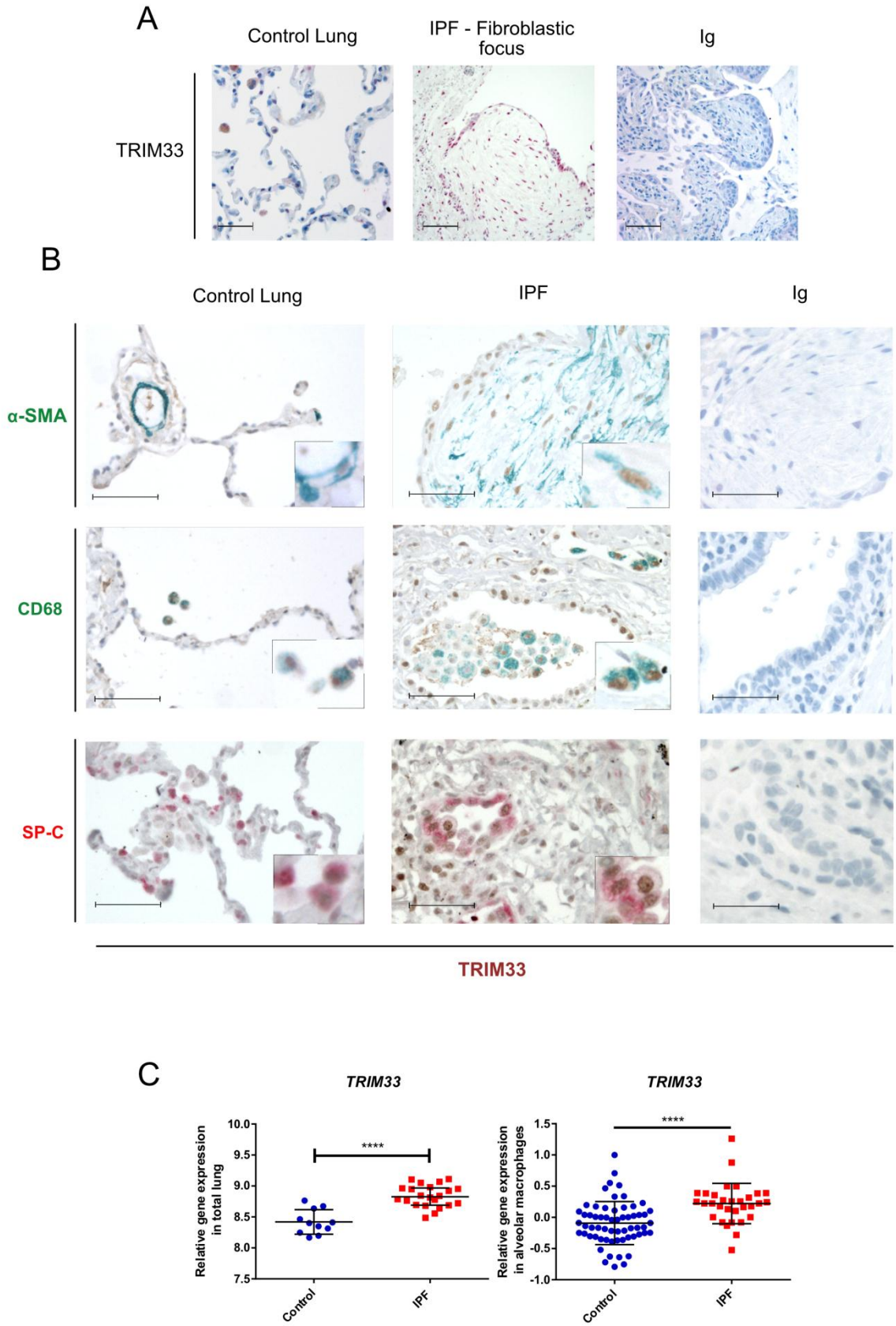
A
Control Lung
IPF - Fibroblastic focus
Ig
TRIM33
B
Control Lung
IPF
Ig
α-SMA
CD68
SP-C
TRIM33
C
TRIM33
TRIM33
Relative gene expression in total lung
Relative gene expression in alveolar macrophages
****
****
10.0
9.5
9.0
8.5
8.0
7.5
1.5
1.0
0.5
0.0
-0.5
-1.0
Control
IPF
Control
IPF

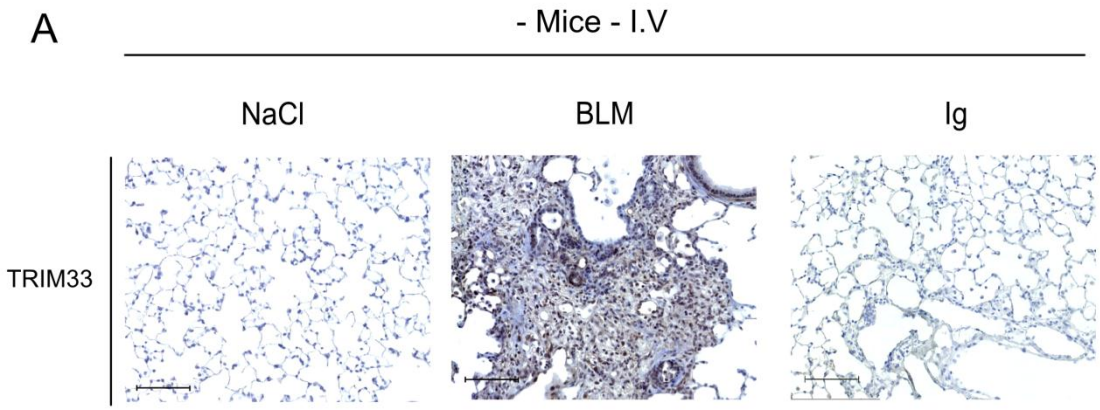
A
- Mice - I.V
NaCl
BLM
Ig
TRIM33

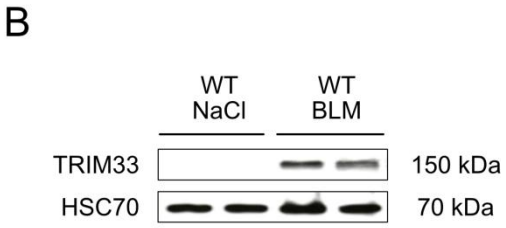
B
WT
NaCl
WT
BLM
TRIM33
150 kDa
HSC70
70 kDa

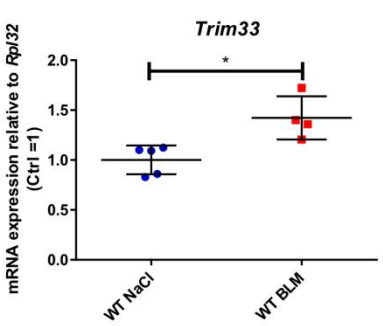
C
Trim33
*
mRNA expression relative to Rpl32
(Ctrl =1)
2.0
1.5
1.0
0.5
0.0
WT NaCl
WT BLM

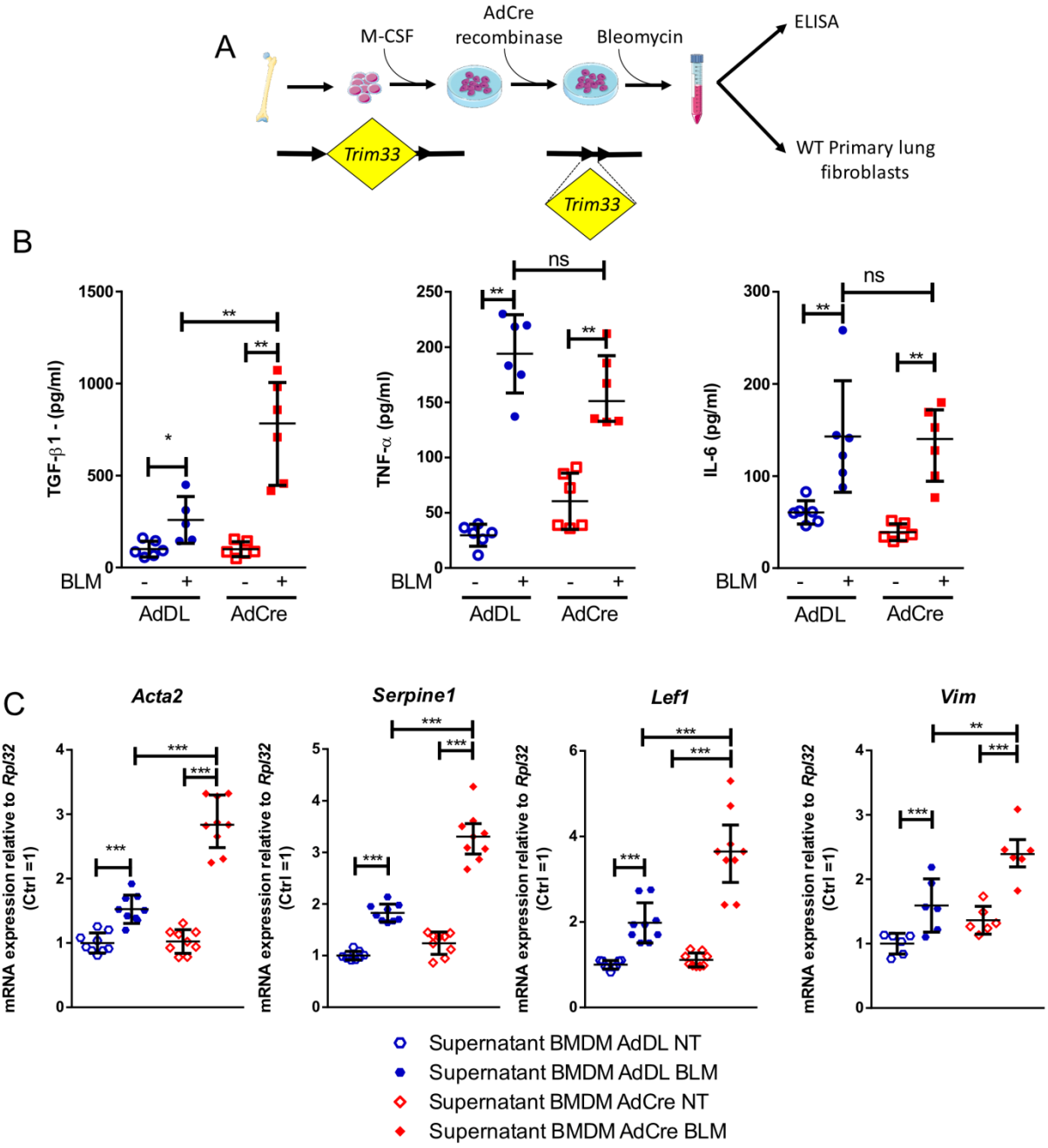
A
M-CSF
AdCre recombinase
Bleomycin
ELISA
WT Primary lung fibroblasts
Trim33
Trim33
B
TGF-β1 - (pg/ml)
TNF-α (pg/ml)
IL-6 (pg/ml)
BLM
AdDL
AdCre
ns
C
Acta2
Serpine1
Lef1
Vim
mRNA expression relative to Rpl32 (Ctrl =1)
Supernatant BMDM AdDL NT
Supernatant BMDM AdDL BLM
Supernatant BMDM AdCre NT
Supernatant BMDM AdCre BLM

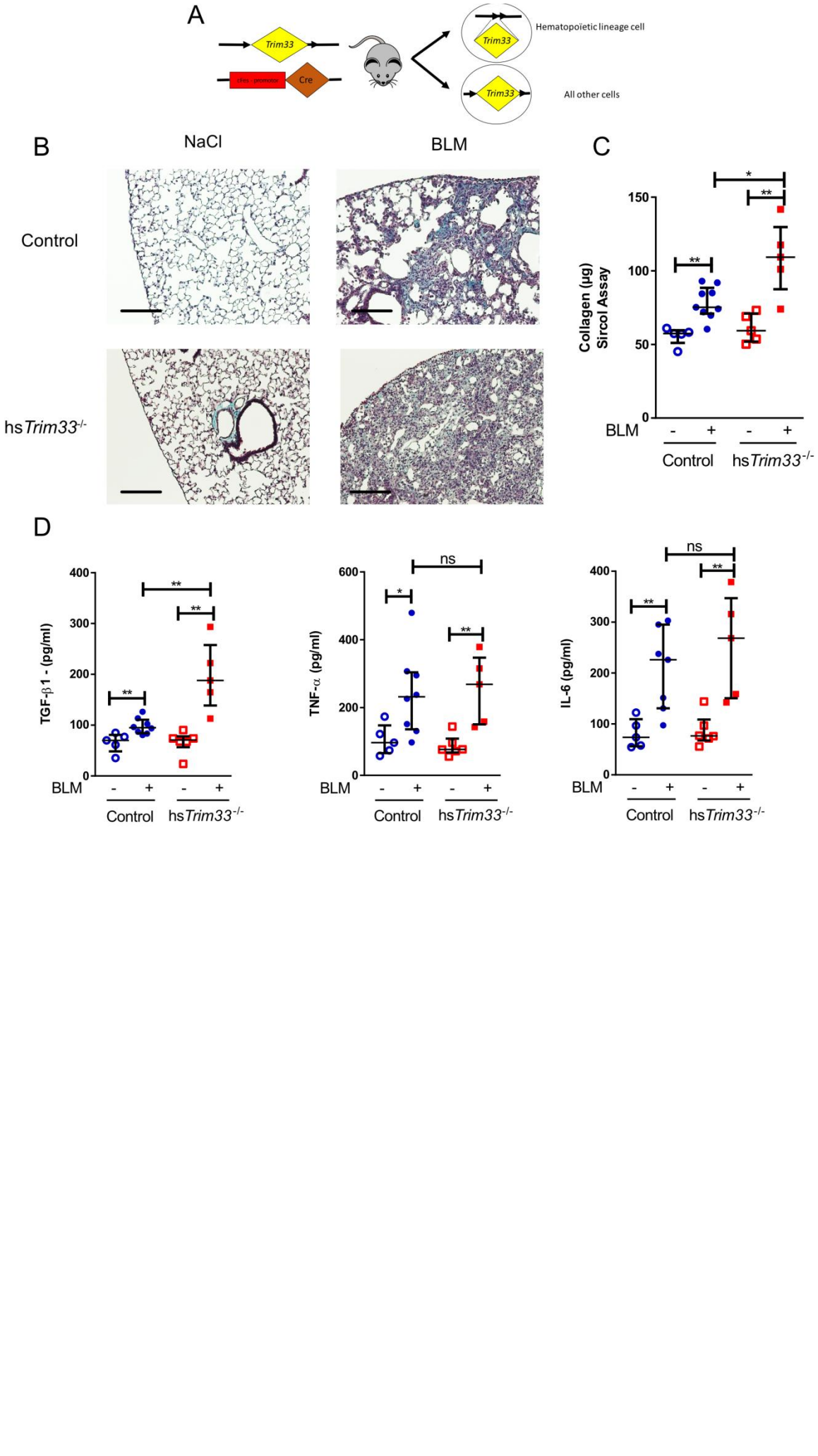
A
Trim33
cRes - promotor
Cre
Hematopoïetic lineage cell
Trim33
All other cells
Trim33
B
NaCl
BLM
Control
hsTrim33-/-
C
Collagen (µg)
Sircol Assay
150
100
50
0
BLM
-
+
-
+
Control
hsTrim33-/-
D
TGF-β1 - (pg/ml)
400
300
200
100
0
TNF-α (pg/ml)
600
400
200
0
IL-6 (pg/ml)
ns
**
*

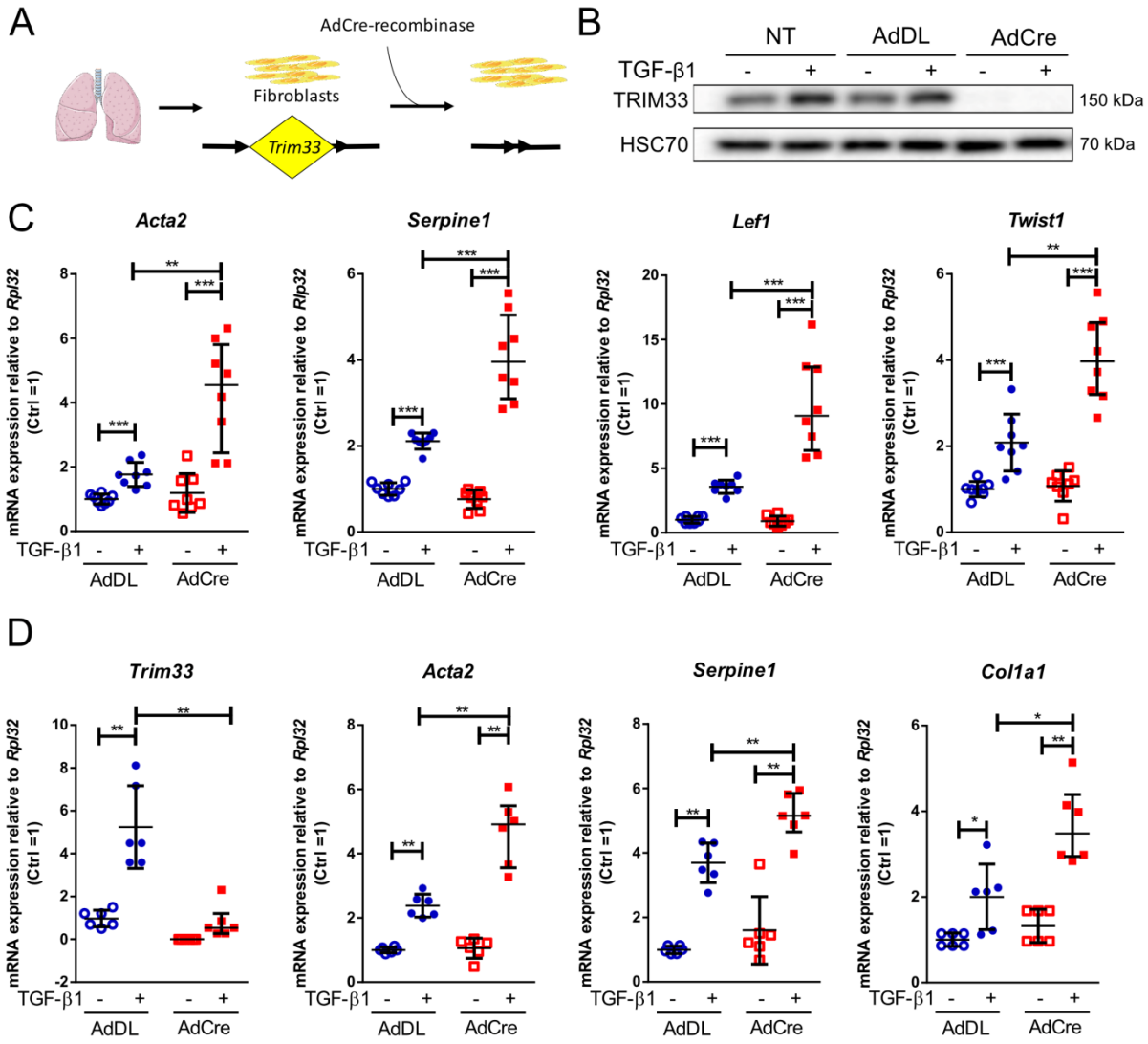
A
AdCre-recombinase
Fibroblasts
Trim33
B
NT
AdDL
AdCre
TGF-β1
TRIM33
150 kDa
HSC70
70 kDa
C
Acta2
Serpine1
Lef1
Twist1
mRNA expression relative to Rpl32 (Ctrl =1)
TGF-β1
AdDL
AdCre
D
Trim33
Acta2
Serpine1
Col1a1

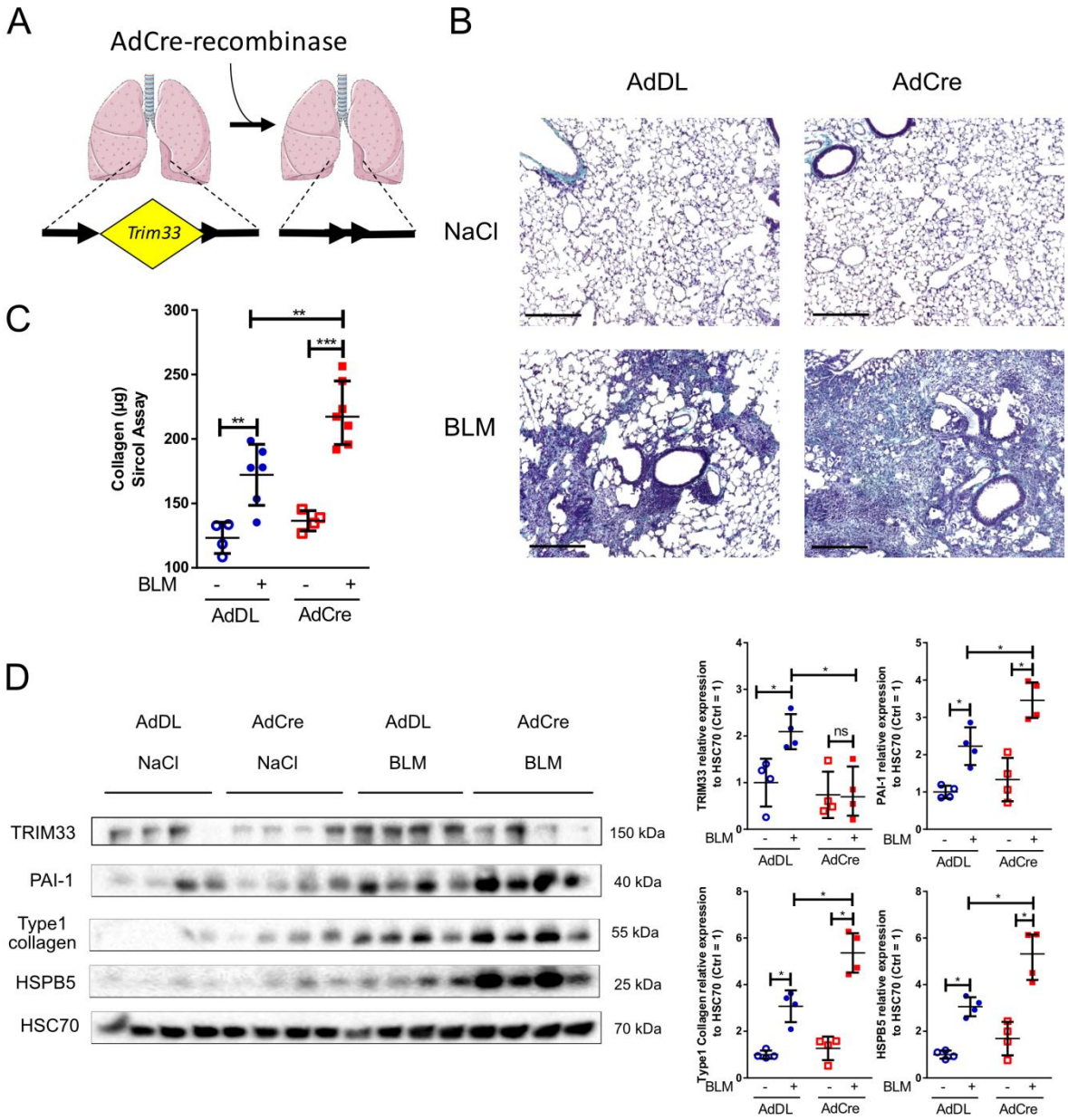
A
AdCre-recombinase
Trim33
B
AdDL
AdCre
NaCl
BLM
C
Collagen (µg)
Sircol Assay
300
250
200
150
100
**
***
**
BLM
-
+
-
+
AdDL
AdCre
D
AdDL
AdCre
AdDL
AdCre
NaCl
NaCl
BLM
BLM
TRIM33
PAI-1
Type1
collagen
HSPB5
HSC70
150 kDa
40 kDa
55 kDa
25 kDa
70 kDa
TRIM33 relative expression
to HSC70 (Ctrl = 1)
PAI-1 relative expression
to HSC70 (Ctrl = 1)
Type1 Collagen relative expression
to HSC70 (Ctrl = 1)
HSPB5 relative expression
to HSC70 (Ctrl = 1)
ns
*

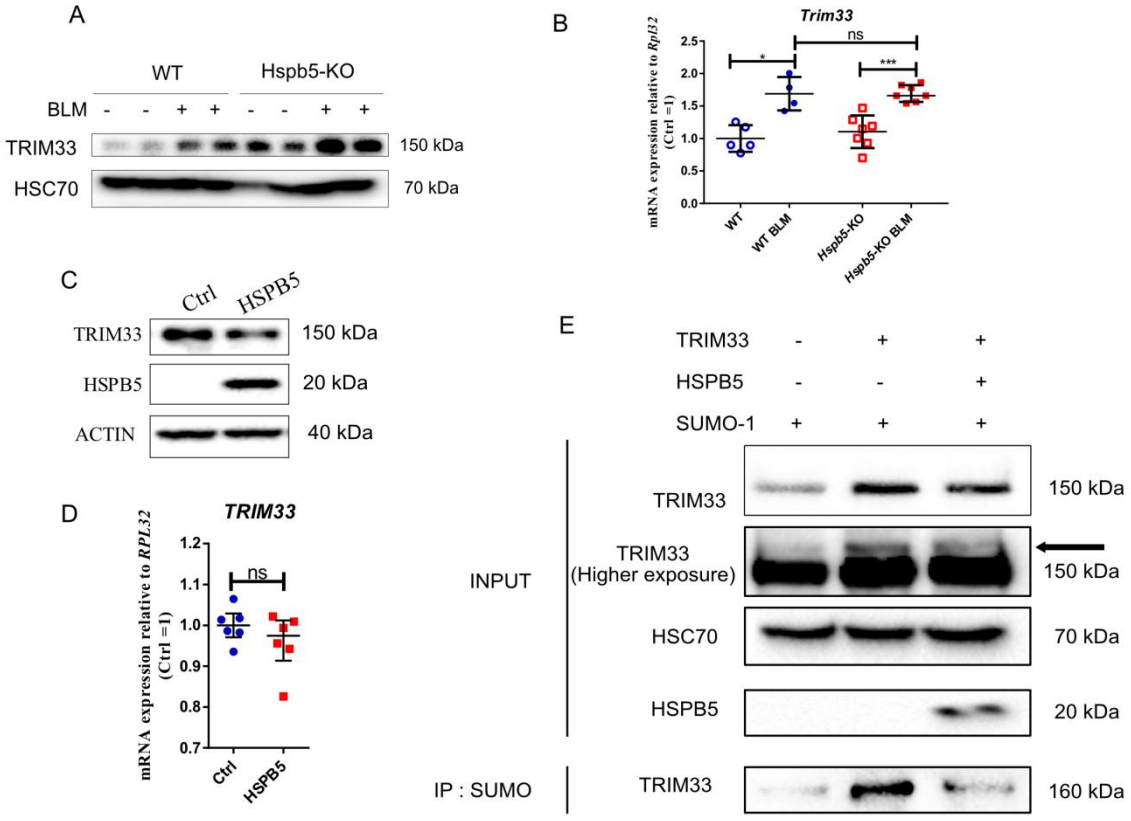
A
WT
Hspb5-KO
BLM - - + + - - + +
TRIM33
HSC70
150 kDa
70 kDa
B
Trim33
ns
*
***
mRNA expression relative to Rpl32 (Ctrl =1)
2.5
2.0
1.5
1.0
0.5
0.0
WT
WT BLM
Hspb5-KO
Hspb5-KO BLM
C
Ctrl
HSPB5
TRIM33
HSPB5
ACTIN
150 kDa
20 kDa
40 kDa
D
TRIM33
ns
mRNA expression relative to RPL32 (Ctrl =1)
1.2
1.1
1.0
0.9
0.8
0.7
Ctrl
HSPB5
E
TRIM33 - + +
HSPB5 - - +
SUMO-1 + + +
INPUT
TRIM33
TRIM33 (Higher exposure)
HSC70
HSPB5
150 kDa
150 kDa
70 kDa
20 kDa
IP : SUMO
TRIM33
160 kDa

Supplemental material and methods

Recombinant adenovirus

The construction of adenoviral vectors has previously been described (1, 2). Briefly, Cre-recombinase cDNA and TGF-β1 cDNA were cloned into a shuttle vector downstream a human CMV promoter and co-transfected with a shuttle plasmid in 293 cells. The control vector (AdDL) with no insert in the E1 region was produced in the same way (1). The TGF-β1 cDNA has cysteine to serine mutations at position 223 and 225, rendering the expressed TGF-β1 biologically active.

Immunochemistry

Paraffin embedded sections of human lung tissue were pretreated in citrate buffer pH6 for 40 minutes for antigen retrieval. Section were then incubated with TRIM33 (sc-101179, Santa Cruz), α-SMA (A2547, Sigma Aldrich) and CD68 (HPA048382, Sigma Aldrich) monoclonal antibody respectively (. Positive cells were revealed using the Chromogen DAB (K3468, Dako) for TRIM33 and Green Chromogen (BRR807A, Biocare Medical Vina Green) or Red Chromogen for CD68, α-SMA, CD326 (WR806, Biocare Medical Warp Red). Rabbit and Mouse Ig were used to test the specificity of immunostaining.

Immunofluorescence

The lungs from mice were insufflated with a mix of 1:1 Water/OCT and quickly freeze at -80°C. Slide from those lungs were fixed in methanol for 15 min before being saturated in 5%

FBS. Primary antibodies were incubated over-night at 4°C for TRIM33 (301-059A Biothyl laboratory, Texas, USA), Vimentin (ab8978, Abcam), CD68 (NPB2-33337, Novus Bio), GFP (#2956), CD326 (ab221552, abcam), ER-TR7 (NB100-64932, Novus Bio). Goat anti-rabbit and goat anti-mouse conjugated with Alexa Fluor 594 or Alexa Fluor 488 (Molecular Probe, InVitrogen, Cergy Pontoise, France) were used as secondary antibodies at a dilution of 1 : 2000.

TGF- β1, TNFα, IL-6 quantification (ELISA)

Total mouse TGF-β1 from BALFs was determined using ELISA (R&D Systems, Lille, France), according to the recommendations of the manufacturer.

Cell culture

A549 lung epithelial cells (ATCC) were grown as monolayers in 5% CO2 at 37°C in DMEM High glucose medium (Lonza, Paris, France), supplemented with 10% of Fetal Bovine Serum (FBS, Lonza). Cells were seeded at 80% confluence one day prior starting the treatment and then stimulated with recombinant human TGF-β1 (rTGF-β1, R&D Systems, Minneapolis, MN) in complete medium at 10 ng/ml.

Primary cell culture

Mouse fibroblasts were isolated as previously described (3, 4) and cultured in DMEM + 10% serum, 1% L-glutamine and 1% penicillin/streptomycin. BMDM were isolated as previously described (5) and cultured in RPMI + 10% serum, 1% L-glutamine and 1% penicillin/streptomycin.

Bone Marrow Isolation and Bone marrow-derived Macrophages

Wild type mice or Floxed *Trim33* mice femurs and tibiae were carefully cleaned of flesh. The tip of each bone was cut off. Then the marrow was collected by inserting a syringe into the medullary cavity at one end of the bone and flushing with Dulbecco's Modified Eagle's Medium (DMEM). The cells were filtered before being centrifuged at 10 000 rpm at 4°C for 10 min. Next the supernatant was replaced by a culture medium DMEM containing macrophage colony-stimulating factor (M-CSF). Cultures were kept at 37°C with 5% CO2 for seven days. The medium was changed every two days.

RNA interference, transfection and infection

Plasmids used were : pcDNA3.1 B myc empty vector, pcDNA3.1 HSPB5, pcDNA3.1 6 his-SUMO-1, pcDNA3.1 TRIM33. TRIM33 was subcloned from pSG5-Flag-TRIM33, a gift from R.Losson (Strasbourg, France). Plasmids constructs were transiently transfected using TransIT-X2® transfection reagent (Mirus bio, Merck KGaA, Darmstadt, Germany) following the manufacturer's recommendations. HSPB5 siRNA and TRIM33 siRNA were purchased from Applied Biosystems (Courtaboeuf, France). SiRNAs (50 nM) were transfected using INTERFERin (Polyplus, Illkirch, France) following the manufacturer's recommendations. Six

hours after transfection, the medium was removed. Adenoviral vectors were used to infect BMDM, primary fibroblasts and 3D-lung tissue slices for 24h with a Multiplicity of infection of 5, 4 and 8 respectively.

q-PCR analysis

Total mRNA from total lungs, mouse fibroblasts and 3D-lung tissue slices was extracted using TRIzol (Invitrogen, Carlsbad, USA). Reverse transcription was performed on total mRNA using the M-MLV kit (Promega, Charbonnieres, France). Quantitative RT-PCR (ViiA 7 Real-Time PCR System, ThermoFischer Scientific, Waktham, USA) was performed on the cDNA using SYBR green master mix (ThermoFisher Scientific) using the following primers for mouse :

Serpine1	Forward	5'-GGCCGTGGAACAAGAATGAGAT-3'
	Reverse	5'-GCTTGAAGAAGTGGGGCATGAAG-3'
Tgfb1	Forward	5'-CGTGGCTTCTAGTGCTGACGC-3'
	Reverse	5'-CCATGTCGATGGTCTTGCAGGT-3'
Hspb5	Forward	5'-GCCTCTTCGACCAGTTCTTCG-3'
	Reverse	5'-AGGGAAGTGGCTGTTGAGAAG-3'
Acta2	Forward	5'-GCAAGAGAGGGATCCTGACG-3'
	Reverse	5'-TCGTCCCAGTTGGTGATGATG-3'
Rpl32 (60S ribosomal protein L32) House keeping gene	Forward	5'-GAAACTGGCGGAAACCCA-3'
	Reverse	5'-GGATCTGGCCCTTGAACCTT-3'
Col1a1	Forward	5'-GCTCCTCTTAGGGGCCACT-3'
	Reverse	5'-CCACGTCTCACCATTGGGG-3'
Twist1	Forward	5'-GGACAAGCTGAGCAAGATTCA-3'
	Reverse	5'-CGGAGAAGGCGTAGCTGAG-3'
Lef1	Forward	5'-TGTTTATCCCATCACGGGTGG-3'
	Reverse	5'-CATGGAAGTGTCGCCTGACAG-3'
Trim33	Forward	5'-CTTCTGCCTGCGCTGTCT-3'
	Reverse	5'-TGCACTTGCATTATCTTCACAA-3'

Or human :

TRIM33	Forward	5′-CTGTTTTCTGCCCTGTACACA -3′
	Reverse	5′-CGCCAGTAGATTCTCAATTGCA-3′
UBC House keeping gene	Forward	5′-GTGGTGCGTCCAGAGAGAC-3′
	Reverse	5′-GGCCTTCGCCATATCCTTTTC-3′

Western blotting

30 µg of proteins were loaded on 12% polyacrylamide gels. Membranes were incubated overnight at 4°C with specific antibodies at a dilution of 1:1000 for the detection of HSPB5 (mouse clone 1B6.1-3G4, Enzo life science, New York, USA), Smad4 (mouse clone B-8, Santa Cruz biotechnologiy, Dallas, USA), TRIM33 (rabbit NBP1-83747, Novus Biologicals, Centennial, USA), PAI-1 (mouse clone 3A120, Thermo Fisher Scientific, Waltham, USA), Col1a1 (HPA008405 Sigma-Aldrich, St. Louis, USA). HSC70 (mouse clone B-6, Santa Cruz Biotechnology) or β-Actin (mouse, a1978, Sigma-Aldrich) antibody was used as a loading control. HRP-conjugated goat anti-rabbit or goat anti-mouse antibodies (Jackson Immunoresearch Laboratories, Suffolk, UK) were used as secondary antibodies.

SUMOylation assay

A549 cells were transfected with 5 µg of each plasmid encoding SUMO-1-his, TRIM33 and HSPB5. Cells were treated overnight with the non-selective DUB inhibitors PR616 (Sigma-Aldrich) before cell lysis. Sumoylated proteins (SUMO-1-His) were pulled-down following the manufacturer's instructions, using Protino ® Ni-NTA agarose (Macherey-Nagel, Bethlehem, USA), an affinity chromatography matrix designed to purifying proteins carrying a His-tag and revealed using TRIM33 antibodies.

FLIM-FRET

Cells were fixed with paraformaldehyde (4% PFA for 10 min) and permeated with a PBS-Triton (0.1%, 5 min) solution. After saturation of nonspecific sites with BSA (5%, 20 min), cells were incubated with primary antibodies overnight in a humidified chamber at 4°C. Cells were stained for SMAD4 with a mouse antibody (clone B-8, Santa Cruz biotechnology), and for TRIM33 with a rabbit antibody (NBP1-83747). Goat anti-rabbit and goat anti-mouse conjugated with Alexa Fluor 594 and Alexa Fluor 488 respectively (Molecular Probe, InVitrogen, Cergy Pontoise, France) were used as secondary antibodies at a dilution of 1: 2000.

The interaction between Smad4 and TRIM33 was studied using FLIM-FRET measurements. The fluorescence lifetime is defined as the average time a molecule remains in an excited state prior to return to the ground state. Fluorescence lifetime imaging microscopy (FLIM) is a well-established technique to study molecular interactions and visualize FRET. The

presence of acceptor molecules in the close environment of the donor allows FRET to occur, resulting in a decrease of donor fluorescence lifetime.

We have measured the fluorescence lifetime of Smad4-Alexa 488 (donor) in the presence and the absence of TRIM33-Alexa 494 (acceptor) to determine the occurrence of FRET. Imaging was carried out with a ×100 PlanApo objective (NA: 1.4, oil, Nikon, Japan) using a time-correlated single-photon counting (TCSPC) module (PicoQuant) on a Nikon Eclipse TE-200 confocal scanning microscope from DImaCell imaging facility (Dijon, France). Excitation at 485 nm was provided by a pulsed diode laser (40 MHz). Fluorescence emission of Alexa 488 was collected using a Single-Photon Avalanche Diode detector, using a FF01-520/35 band-pass emission filter (Semrock). We performed a global lifetime analysis on regions of interest of the FLIM images using the SymPhoTime software (PicoQuant). Fluorescence lifetimes were calculated by fitting the tail of Alexa 488 fluorescence decay with a bi-exponential model, with two lifetime constants. For this analysis, we used the mean value of these two constants as the Alexa 488 lifetime.

Bio Layer Interferometry

For in vitro interaction assays, we used Biolayer interferometry technology (Octet Red96, Forté-Bio). This is an optical analytical technique that analyzes the interference pattern of white light reflected from biosensor tip surface. The change in thickness of the biological layer resulting from analyte binding on his immobilized ligand was measured by a wavelength shift.

BLI was performed using an OctetRED96 instrument from PALL/ForteBio (San Jose, USA). Recombinant SMAD4 and HSPB5 were biotinylated with NHS-PEG4-biotin reagent (Thermo Fisher Scientific, 21330) in a ratio of 1:3. The excess of reagent was removed using Zeba Spin Desalting Columns (Thermo Fisher Scientific). Proteins were loaded on streptavidin biosensors (ForteBio) at 5µg/ml. Association step was performed for 600 sec in wells containing the indicated concentration of rhSMAD4 or rhTRIM33 diluted in PBS. The experiment was performed in black 96-well plates with 200 µL volume/well, under constant shaking (400 g) at 25°C. The Kd values were calculated by the software provided by the manufacturer (version 7.1.0).

Supplemental Reference

1. Bett AJ, Haddara W, Prevec L, Graham FL. An efficient and flexible system for construction of adenovirus vectors with insertions or deletions in early regions 1 and 3. *Proceedings of the National Academy of Sciences of the United States of America* 1994;91:8802-8806.
2. Sime PJ, Xing Z, Graham FL, Csaky KG, Gauldie J. Adenovector-mediated gene transfer of active transforming growth factor-beta1 induces prolonged severe fibrosis in rat lung. *The Journal of clinical investigation* 1997;100:768-776.
3. Bonniaud P, Martin G, Margetts PJ, Ask K, Robertson J, Gauldie J, Kolb M. Connective tissue growth factor is crucial to inducing a profibrotic environment in "fibrosis-resistant" balb/c mouse lungs. *American journal of respiratory cell and molecular biology* 2004;31:510-516.
4. Janssen LJ, Farkas L, Rahman T, Kolb MR. Atp stimulates ca(2+)-waves and gene expression in cultured human pulmonary fibroblasts. *The international journal of biochemistry & cell biology* 2009;41:2477-2484.
5. Lv J, Xiong Y, Li W, Yang W, Zhao L, He R. Blt1 mediates bleomycin-induced lung fibrosis independently of neutrophils and cd4+ t cells. *The Journal of Immunology* 2017:1600465.

Supplemental Figure 1 : TRIM33 is up-regulated in lung of IPF patients. mRNA levels of TRIM33 were analyzed by quantitative PCR of samples from 27 IPF patients undergoing lung transplantation and 29 normal lung tissues flanking lung cancer resections (Control). Results are expressed as median with interquartile range; **P = 0.0028, unpaired t test with Welch's correction.

Supplemental Figure 2: TRIM33 is up-regulated in rodent models of experimental lung fibrosis.(A) Representative images of TRIM33 immunostaining on lung sections from mice challenged with either intratracheal instillation of bleomycin (BLM) (upper left), or intrapleural administration of AdTGF-ß1 (upper right) or from rats exposed to AdTGF-ß1 by intrapleural injection (lower part), scale bar 250 µm. (B) Representative images (n=5) of TRIM33 immunofluorescence (red) with a co-staining of either Vimentin (Green) for fibroblasts (arrow head) or CD68 (Green) for macrophages (arrow head) on lung sections from mice 21 days after instillation of bleomycin, scale bar: 10 µm.

Supplemental Figure 3: Trim33 deletion does not affect cytokine expression in BMDM. (A-B) mRNA levels of Trim33, Tgfb1 were analyzed by quantitative PCR on BMDM infected with AdDL or AdCre and exposed to bleomycin (5mg /ml, 48h) (n=3). (C) Viability of BMDM assessed using methylene blue after bleomycin treatment (5mg/ml, 48h). Results are expressed as median with interquartile range (n=3 with 2 biological duplicates). (D) Cytokine array was performed on the supernatant from BMDM infected with AdDL or AdCre and exposed to bleomycin (5mg /ml, 48h) (n=3).

Supplemental Figure 4: hsTrim33-/- mice are more sensitive to bleomycin-induced fibrosis. (A) Collagen quantification of lung sections stained with Picrosirius red from control and hsTRIM33-/- mice at day 21 after BLM-treatment. Results are expressed as median with interquartile range; *P< 0.05, **P< 0.01, non-parametric Mann-Whitney test, n= 4-8 per group. Measurements were made on the parenchyma areas. (B) Acta2 mRNA levels analyzed by quantitative PCR in lungs from control and hsTrim33-/- mice at day 21 after BLM-treatment. Results are expressed as median with interquartile range. *P < 0.05, **P < 0.01, non-parametric Mann-Whitney test, n= 4-8 per group.

Supplemental Figure 5: hsTrim33-/- mice are more sensitive to intravenous bleomycin-induced fibrosis. (A) Histological analysis of control (hsTrim33-/-) and hsTrim33-/- mouse lungs 14 days after intravenous injection of bleomycin (BLM). Hematoxylin and eosin staining (n= 6), scale bar 250 µm. (B) Collagen quantification using lung sections stained with Picrosirius red from control and hsTrim33-/- mice at day 14 after BLM exposure. Measurements were made on the parenchyma areas. Results are expressed as median with interquartile range. **P< 0.01, non-parametric Mann-Whitney test; n= 7-9 per group. (C) Representative images (×500) of a-SMA immunostaining on lung sections from control and hsTrim33-/- mice at day 21 after BLM-treatment, scale bar: 250 µm.

Supplemental Figure 6: Intra-tracheal injection of AdCre allows creation of a partial Trim33 lung knock-out. (A) Cytometry analysis on the YPF signal on cells from whole lung of R26-stop-EYFP mutant mice lung, 3 days after AdDL or AdCre intra-tracheal injection (n=3). (B) Representative images (×300) of YFP immunofluorescence (Yellow) on lung sections from mice 3 days after instillation of AdCre (n=3), scale bar: 20 µm. (B) Representative images (×500) of YFP immunofluorescence (Yellow) with a co-staining of either CD326 (Red) for epithelial cells or ER-TR7 (Red) for fibroblast or CD68 (Red) for macrophages on lung sections from mice 3 days after instillation of AdCre (n=3), scale bar: 10 µm.

Supplemental Figure 7: Pulmonary inhibition of Trim33 worsens bleomycin-induced fibrosis in mice. (A) mRNA levels of Col1a1, Serpine1 and Twist1 were analyzed by quantitative PCR in the lungs from control and Trim33f/l mice exposed to AdDL or AdCre and day 21 after bleomycin (BLM) or NaCl instillation. Results are expressed as median with interquartile range. *P < 0.05, **P < 0.01, non-parametric Mann-Whitney test, n= 4-8 per

group. (B) May-Grünwald Giemsa quantification of the BALF cells isolated from mice, 3 days after injection with either NaCl, AdDL or AdCre (n=3 per group).

Supplemental Figure 8: TRIM33 is able to interact directly with SMAD4. (A) Hspb5 mRNA levels analyzed by quantitative PCR in lungs from control and Hspb5-KO mice at day 21 after BLM-treatment. Results are expressed as median with interquartile range. *P < 0.05, non-parametric Mann-Whitney test, n= 4-8 per group. (B) Protein levels of TRIM33 analyzed by Western Blot in primary pulmonary fibroblasts from SV129 control mice of SV129 Hspb5 deficient mice (Hspb5-KO) cultured with rTGF-ß1 (48h, 10ng/ml) (n=3). (C) The binding of recombinant TRIM33 to recombinant HSPB5 immobilized on a SA biosensor was determined by biolayer interferometry (graph representative of 3 independent experiments). (D) The binding of recombinant SMAD4 to a recombinant TRIM33 immobilized on a SA biosensor was determined by biolayer interferometry (graph representative of 3 independent experiments). (E) The proximity between TRIM33 and SMAD4 was asset by FLIM-FRET in A549 cells transfected with HSPB5 or an empty vector as control (Ctrl). The fluorescence lifetime of SMAD4 (Alexa 488, donor) in presence or the absence of TRIM33 (Alexa 494, acceptor) was determined to assess FRET (n=3). Results are shown as median with interquartile range; ***P < 0.001, non-parametric Mann-Whitney test. N.S; nonsignificant.

Supplemental Figure 9: uncropped Western Blots.

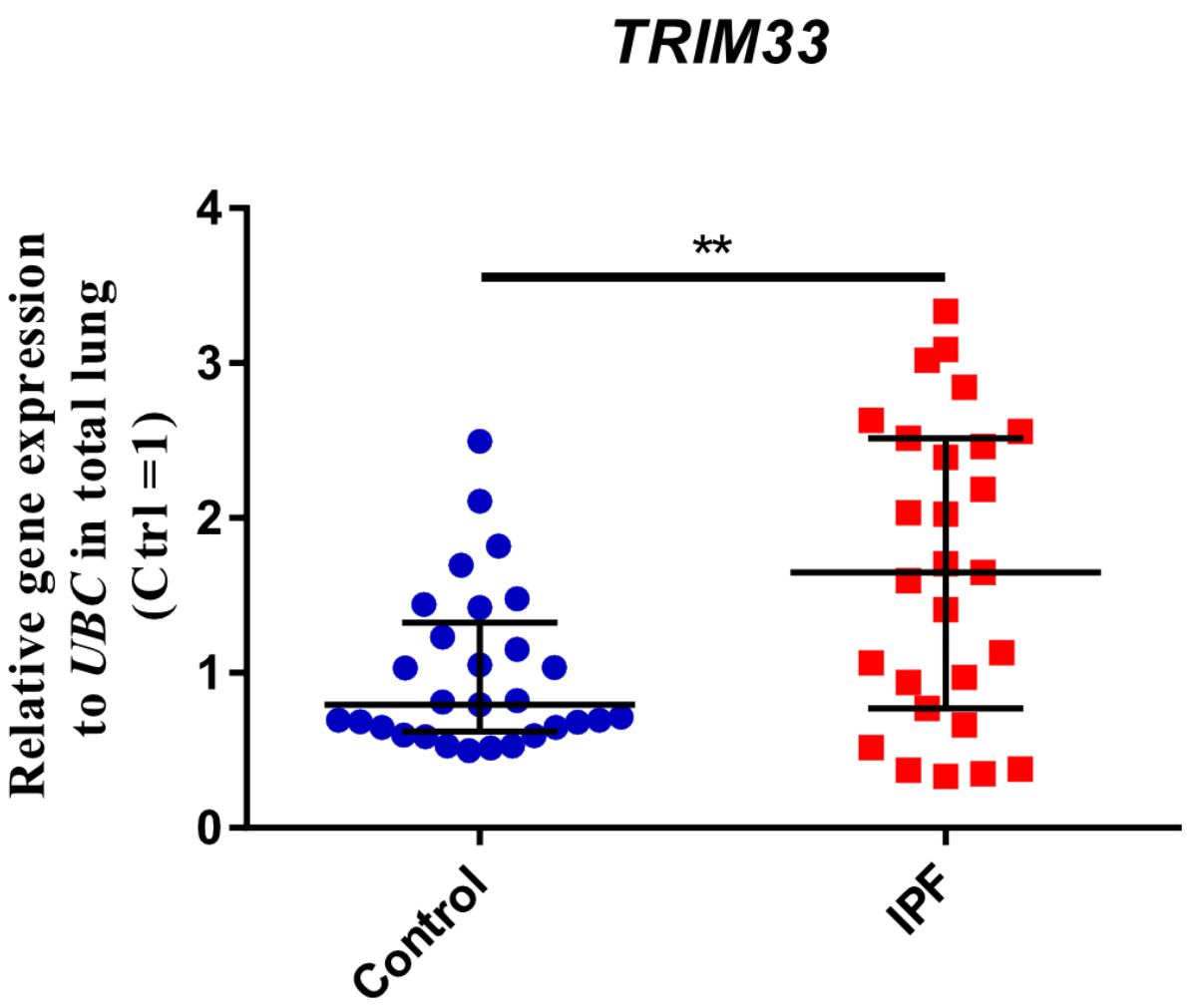
TRIM33
Relative gene expression to UBC in total lung (Ctrl =1)
4
3
2
1
0
**
Control
IPF

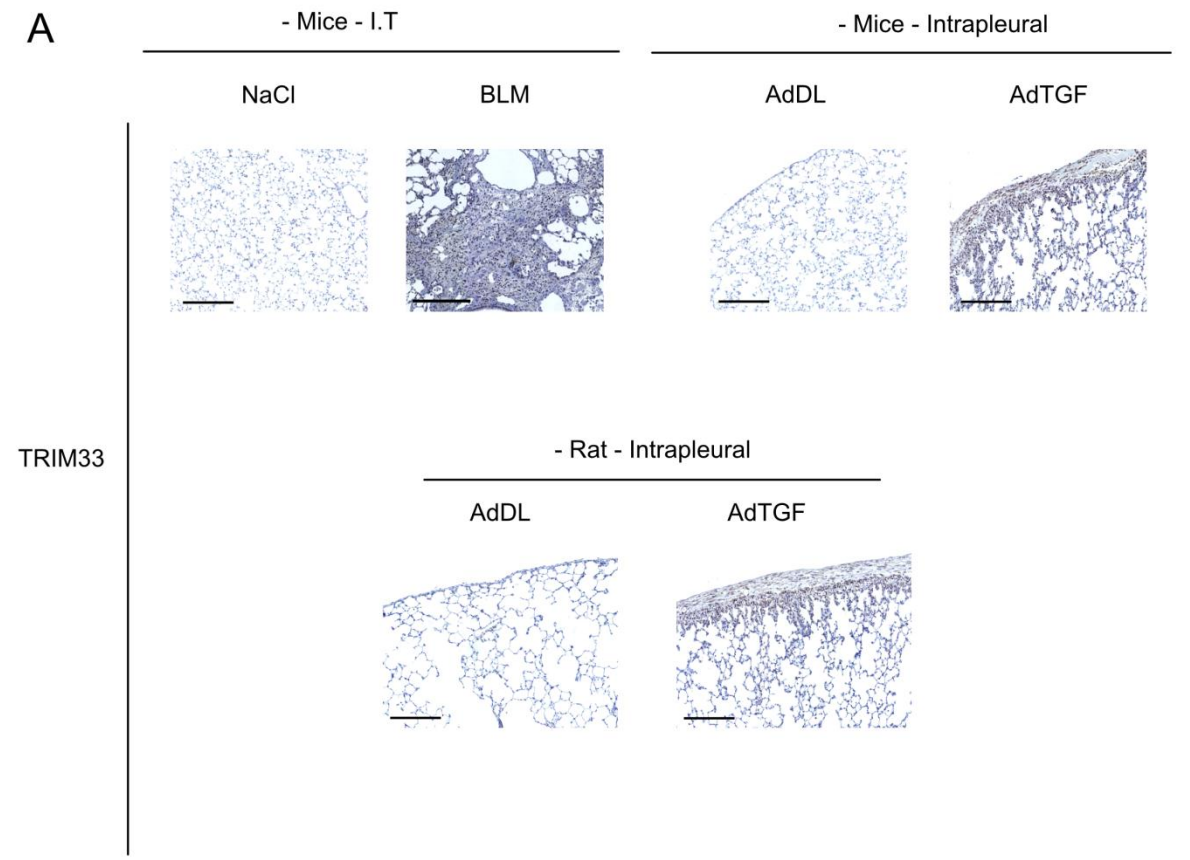
A
- Mice - I.T
- Mice - Intrapleural
NaCl
BLM
AdDL
AdTGF
TRIM33
- Rat - Intrapleural
AdDL
AdTGF

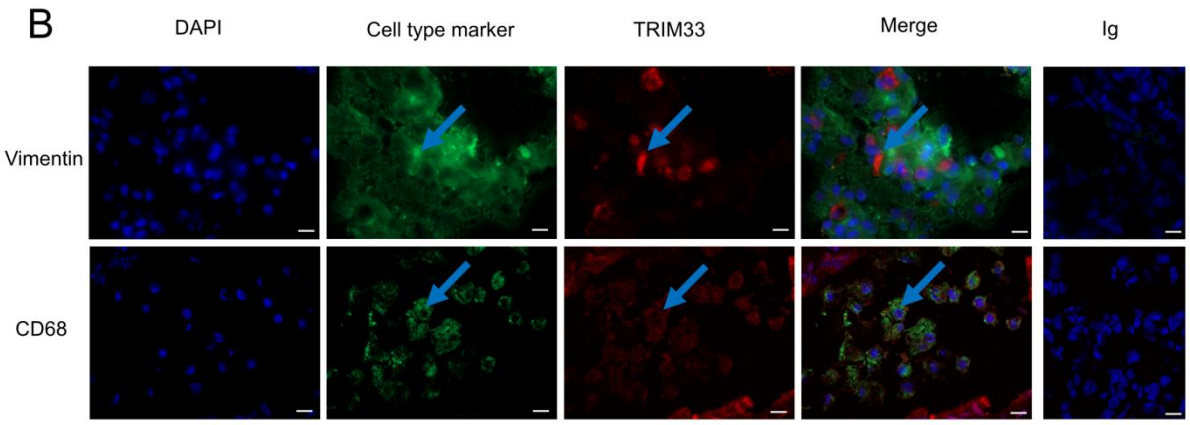
B
DAPI
Cell type marker
TRIM33
Merge
Ig
Vimentin
CD68

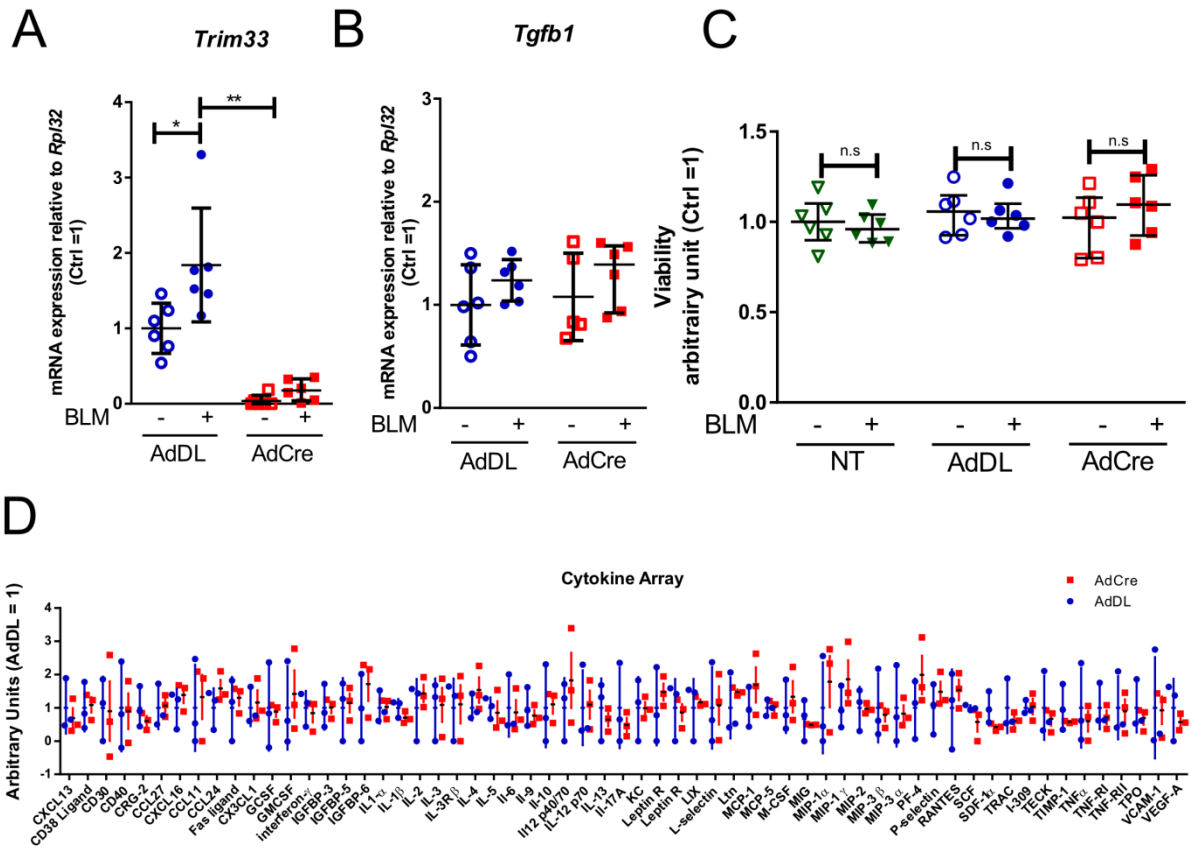
A
Trim33
mRNA expression relative to Rpl32 (Ctrl =1)
BLM
AdDL
AdCre
B
Tgfb1
mRNA expression relative to Rpl32 (Ctrl =1)
C
Viability arbitrairy unit (Ctrl =1)
n.s
NT
AdDL
AdCre
D
Cytokine Array
Arbitrary Units (AdDL = 1)
AdCre
AdDL
CXCL13
CD38 Ligand
CD30
CD40
CRG-2
CCL27
CXCL16
CCL11
CCL24
Fas ligand
CX3CL1
GCSF
GM-CSF
IGFBP-3
IGFBP-5
IGFBP-6
IL-2
IL-3
IL-4
IL-5
Il-6
Il-9
Il-10
Il12 p40/p70
IL-12 p70
IL-13
Il-17A
KC
Leptin R
LIX
L-selectin
Ltn
MCP-1
MCP-5
M-CSF
MIG
MIP-2
P-selectin
RANTES
SCF
TRAC
I-309
TECK
TIMP-1
TNF-RI
TNF-RII
TPO
VCAM-1
VEGF-A

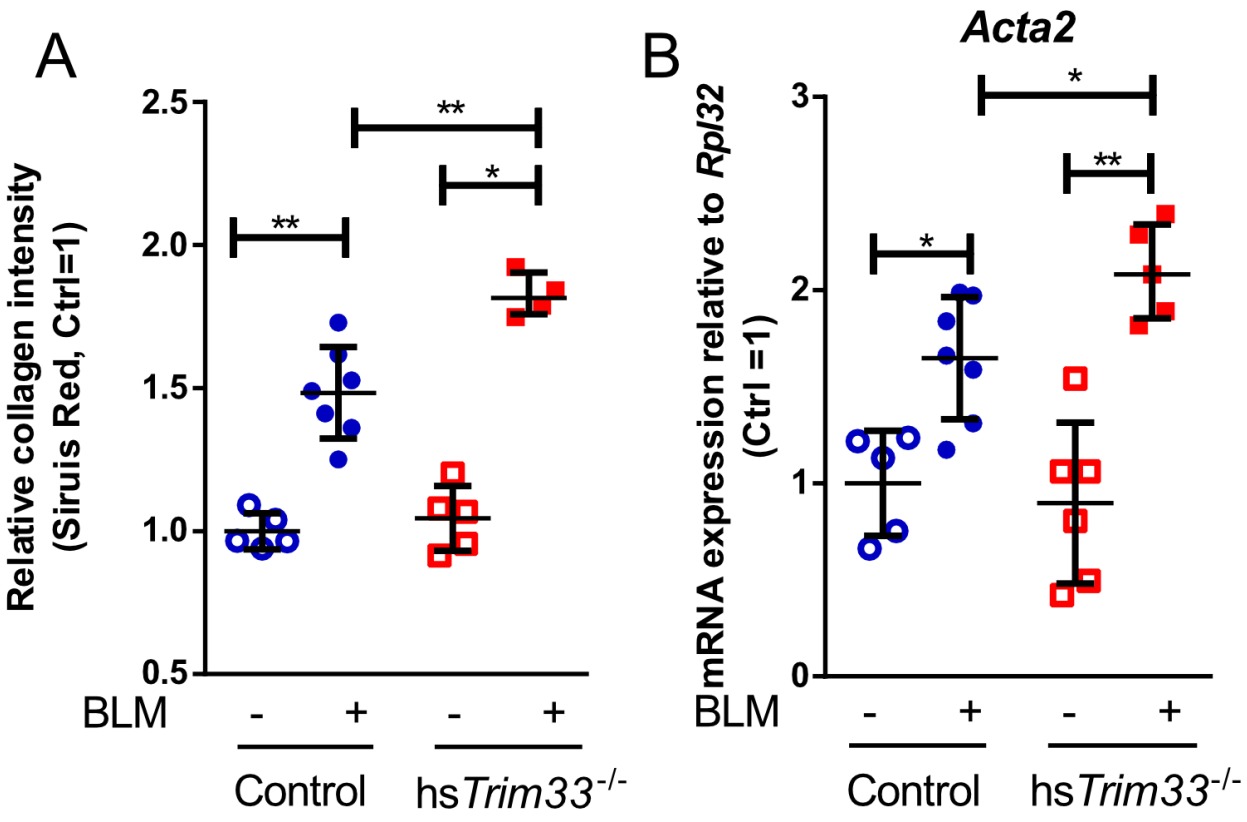
A
Relative collagen intensity
(Siruis Red, Ctrl=1)
2.5
2.0
1.5
1.0
0.5
**
**
*
BLM
-
+
-
+
Control
hsTrim33-/-
B
Acta2
mRNA expression relative to Rpl32
(Ctrl =1)
3
2
1
0
*
*
**
BLM
-
+
-
+
Control
hsTrim33-/-

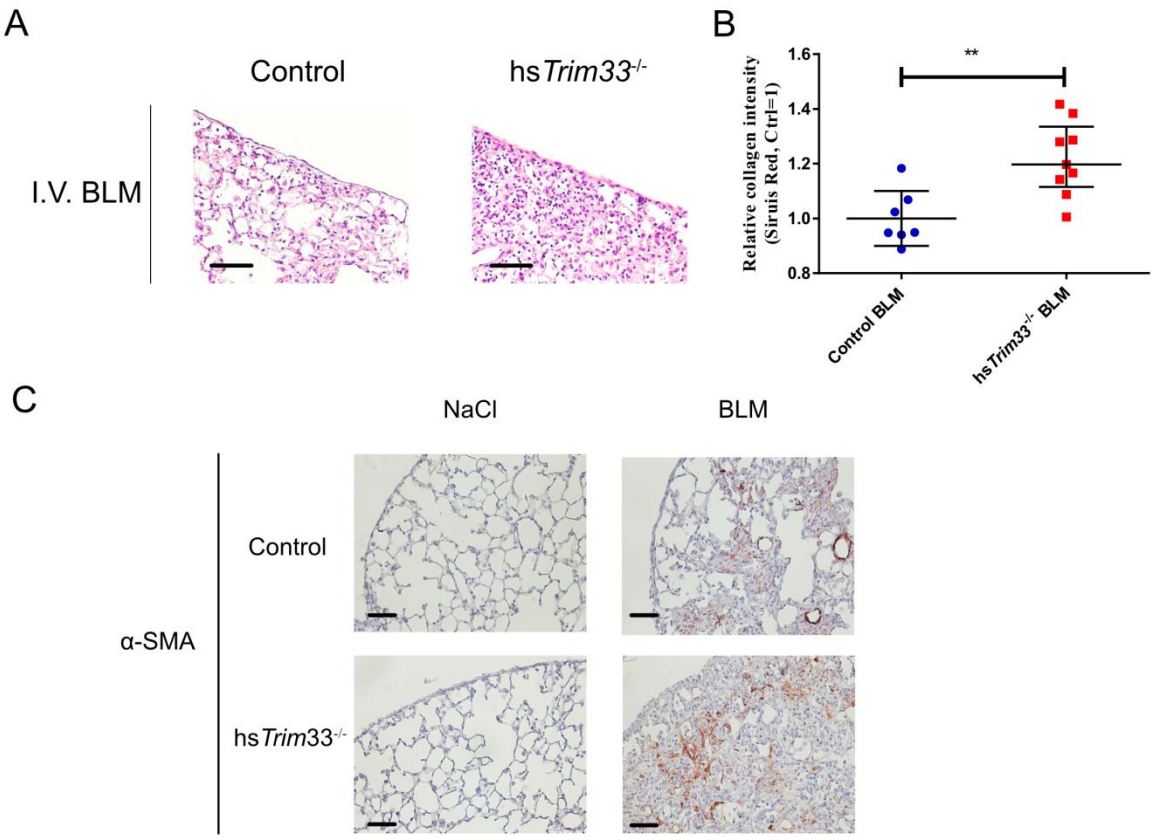
A
Control
hsTrim33-/-
I.V. BLM
B
Relative collagen intensity (Sirius Red, Ctrl=1)
1.6
1.4
1.2
1.0
0.8
**
Control BLM
hsTrim33-/- BLM
C
NaCl
BLM
Control
α-SMA
hsTrim33-/-

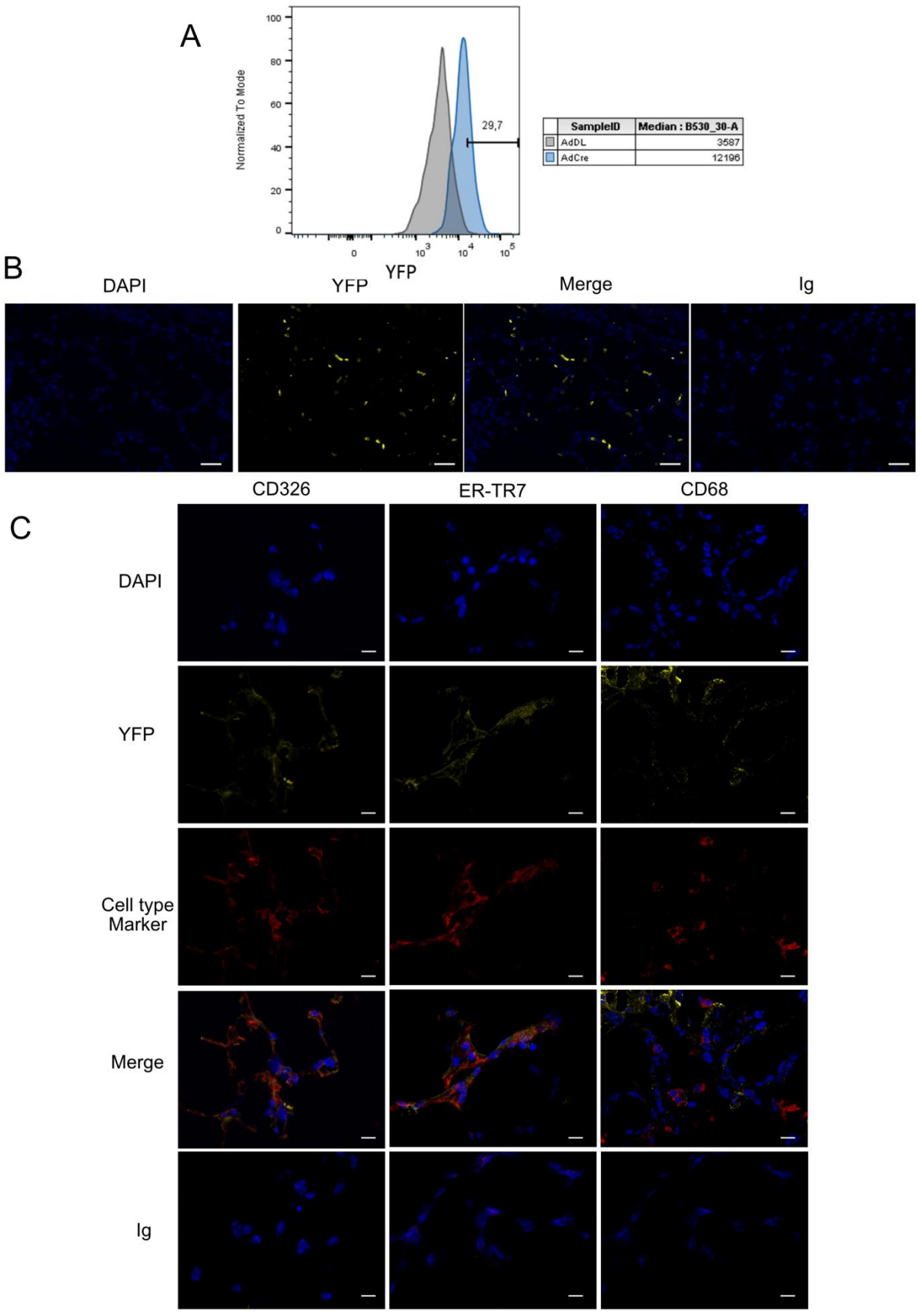
A
Normalized To Mode
100
80
60
40
20
0
29,7
0
10^3
10^4
10^5
YFP
SampleID | Median : B530_30-A
AdDL | 3587
AdCre | 12196
B
DAPI
YFP
Merge
Ig
C
CD326
ER-TR7
CD68
DAPI
YFP
Cell type Marker
Merge
Ig

A

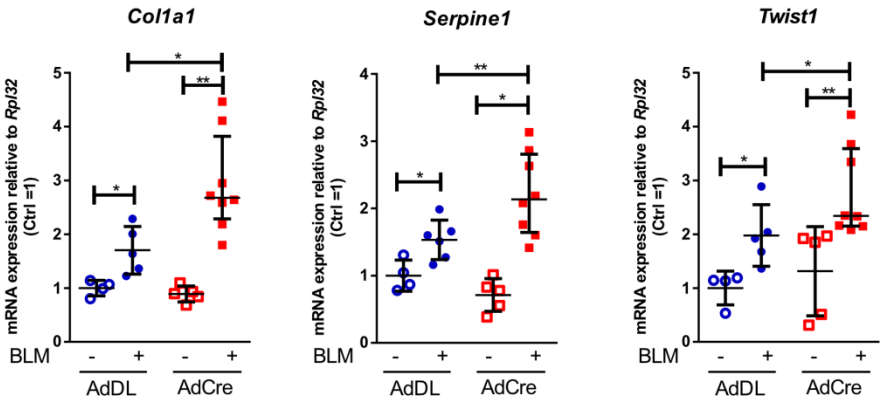
Col1a1
Serpine1
Twist1
mRNA expression relative to Rpl32 (Ctrl =1)
BLM
AdDL
AdCre

B

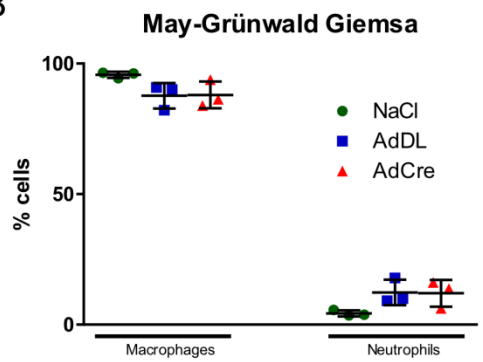
May-Grünwald Giemsa
% cells
NaCl
AdDL
AdCre
Macrophages
Neutrophils

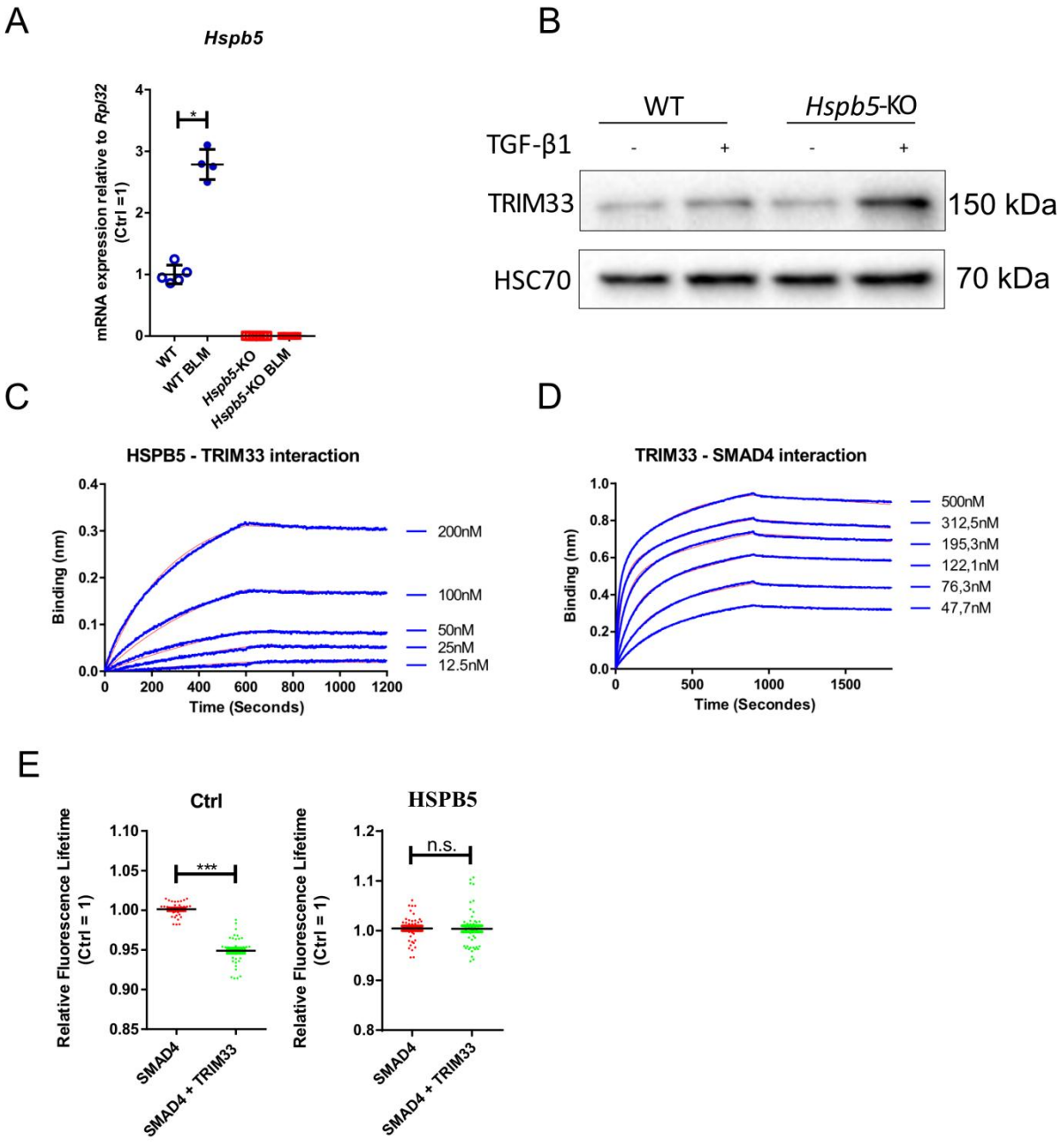
A
Hspb5
mRNA expression relative to Rpl32 (Ctrl =1)
*
WT
WT BLM
Hspb5-KO
Hspb5-KO BLM
B
WT
Hspb5-KO
TGF-β1
-
+
-
+
TRIM33
150 kDa
HSC70
70 kDa
C
HSPB5 - TRIM33 interaction
Binding (nm)
Time (Seconds)
200nM
100nM
50nM
25nM
12.5nM
D
TRIM33 - SMAD4 interaction
Binding (nm)
Time (Secondes)
500nM
312,5nM
195,3nM
122,1nM
76,3nM
47,7nM
E
Ctrl
HSPB5
Relative Fluorescence Lifetime (Ctrl = 1)
***
n.s.
SMAD4
SMAD4 + TRIM33

Fig 2 B - TRIM33

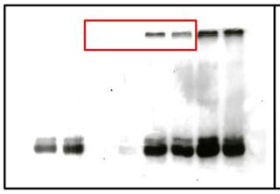

Fig 2 B - HSC70

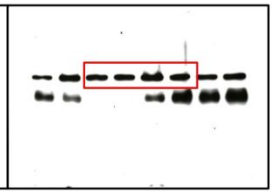

Fig 5 B TRIM33

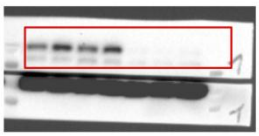

Fig 5 B HSC70

Fig 6 D TRIM33

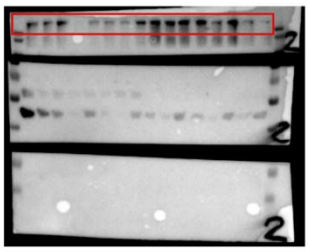

Fig 6 D HSC70

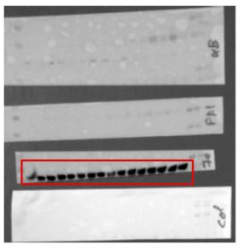

Fig 6 D HSPB5, PAI-1, Type1 Collagen

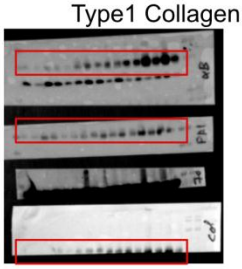

Fig 7 A TRIM33

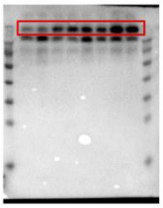

Fig 7 A HSC70

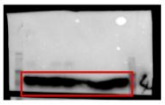

Fig 7 C TRIM33, ACTIN HSPB5

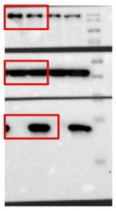

Fig7 E TRIM33

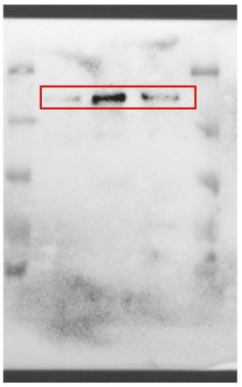

Fig7 E HSC70, HSPB5

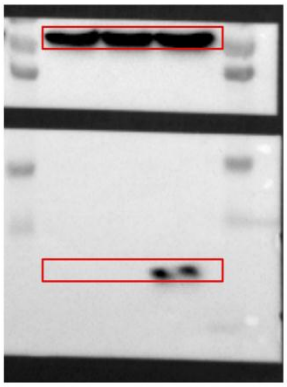

Fig7 E TRIM33

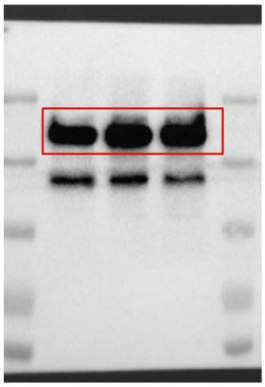

S8 - TRIM33 - HSC70